Review of the first revised version of

"Implementation and assessment of a carbonate system model (Eco3M-CarbOxv1.1) in a highly-dynamic Mediterranean coastal site (Bay of Marseille, France)"

submitted for publication to Geoscientific Model Development
by K. Lajaunie-Salla and co-authors

General reply: We thank again the Reviewer Dr Munhoven for his second evaluation of our work. We thank too him for the detailed and useful comments that contributed to greatly improve the manuscript. We consider all of his comments to improve the manuscript.

1. General comments

The authors' reply the revised manuscript are not very "reviewer-friendly." It is nowadays standard practice to provide a "track change" (or a LATEXDIFF) version of the manuscript clearly identifying the changes made to the text, right in the text. The equivalent information is seemingly given in the reply, except that the line numbers provided there do not match, so that one has to search manually for the exact location of the changes.

The preparation of the manuscript would also have benefited from some extra care. Page numbers restart at 1 after page 23 without any apparent reason.

Reply : The preparation of the revised ms has been reviewed with care and page numbers have been reprocessed. A new check of the different sections has been carefully performed.

1.1 Appreciation of the replies to reviewers

The authors have all in all well responded to the referees' comments, with one exception though. In the response to my comment 2.3, regarding the missing effect of river intrusions on DIC — TA perturbations are taken into account, but as these are carried mainly by $HCO3^-$, they also generate DIC perturbations of the same magnitude, which are neglected — I read at the top of the fourth page (page numbers in the response would have been helpful) that

"Concerning the riverine inputs scenarii, we decide to focus on nitrate and alkalinity supply. In fact the model simulates the DIC increases, as is observed, which highlight that the carbonate system module is well resolved."

The reply to the comments is somewhat ambiguous as suggests that DIC changes are taken into account, while they are actually not, as stated in the manuscript at lines 413–414 :

" [. . .] the experimental design on the Rhône River supply only considers the TA perturbation on the carbonate system but not that due to the DIC supply."

So, even if the model reproduces the observed DIC increases (as stated in the reply), this must obviously be for the wrong reasons, as only one half of the effects of the perturbation due to river intrusions is taken into account. By the way, no one argued that the carbonate system module was not well resolved.

Reply : We decided to remove the scenario of AT supply by river and all the text refered to it in the methods and results/discussion sections. See our detailed comment on this point hereafter.

1.2 Appreciation of the revised manuscript

The model description has been improved and the rationale behind the carbonate speciation calculations is now presented in a new appendix. Unfortunately, the layout of that appendix is rather chaotic which makes it difficult to read.

2. Specific comments

2.1 River intrusion experiments: poor justification

The justification added at lines 414–417 for taking the effect of river intrusions into account only in terms of the resulting TA but not DIC perturbations is rather cavalier and scientifically untenable. This is a completely unrealistic assumption that makes the outcome of the experiment meaningless and thus essentially invalidates any conclusion drawn from it.

I only see two options to address this shortcoming:
1. the river intrusion experiments are repeated with the effect on DIC included (which should be rather straightforward to correct) and the discussion of the results adapted;
2. these experiments are simply taken out of the paper as the current results are essentially unfounded.

Even in preliminary experiments, one must not chose to disregard one of two effects of a perturbation if these are of the same order of magnitude. Such arbitrary choices lead to arbitrary results.

Reply : We have chosen the second option proposed by the Reviewer. Mainly because it was not straightforward to consider DIC supply by River as considered for AT. In fact DIC is not as conservative as AT is regard to salinity. It is then impossible to use a relationship between DIC and salinity as that used between AT and salinity in the previous version of our manuscript. In the context of a 0D modelling developped here, this kind of relationship would have been the only mean to take into account the DIC supply by the Rhône River. In the revised version, we stressed (l 398-401) that rivers also supply TA and DIC and a consideration for these supplies in future works may sensibly modify the modeled carbonate balance in the BoM compared to that presented in this study. Concomitantly we slightly rewrote the end of section 4.1 on the model performance in Discussion.

As noted in the conclusion (l434), a coupling of the Eco3M-CarbOx model to a 3D hydrodynamics model is planed to better represent the complexity of functioning of the BOM. This implementation will enable, for example, to take into account actual DIC and AT supplies from the Rhône River by considering forcing values measured in the River.

3. Technical comments

Reply : All these technical comments have been taken into account in the new revised version of ms.

Page 1, line 22: “the year 2017 that is a period for which” should read “the year 2017 for which”
Page 1, line 25: “of most of variables of carbonate system except Total Alkalinity.” should read “of most of the variables of the carbonate system except for Total Alkalinity.”
Page 1, line 26: “experiments were also conducted” should read “experiments were conducted”
Page 1, line 26: “to (i) seawater” should read “to (i) a seawater”
Page 1, line 27: “Rhône River plume intrusion” should read “Rhône River plume intrusions”; by the way: the name of that river is sometimes spelled “Rhône”, more often “Rhone” — please use the same spelling consistently throughout
Page 1, line 35: “external forcing have” should read “external forcings have”
Page 5, line 188: “a salinity threshold of 37 has been chosen” – is this correct? A threshold of 37 looks rather high to me.
Page 6, line 226: “during MWC period” should read “during the MWC period”
Page 7, line 271: “15 March and 6 May” should either read “15th March and 6th May” or “March 15th and May 6th” (as on line 277, p. 8)

Page 11, line 390: “Moreover, previous study” should read “Moreover, a previous study”, or even better reformulate the sentence to read “Moreover, Fraysse et al. (2013) highlight that . . . ” and discard the citation in brackets.
Page 11, line 402: “a longer period ca. 15 days” should read “a longer period of ca. 15 days”
Page 11, lines 402–403: “high atmospheric pCO2 value and wind speed” better had to read “high atmospheric pCO2 and high wind speeds”
Page 11, line 411: “due to some two” should read “due to two”
29th and 30th pages (pages nr. 6 and 7), throughout: “in the pH scale” should read “on the pH scale”
29th page (page nr. 6): “Concentration in Total Fluoride (TF) ions” should read “Total Fluoride concentration” (without “ions,” as TF includes the non ionic HF)
29th page (page nr. 6): “Concentration in Total Sulphate (TS) ions” should read “Total Sulphate concentration” (“ions” is superfluous)
29th page (page nr. 6): “Concentration in Total Boron (TB)” should read “total boron concentration” (without “ions,” as TB includes the non ionic B(OH)3)
29th page (page nr. 6): KF is the dissociation constant of hydrogen fluoride (or of hydrofluoric acid), not of fluoride ions
29th page (page nr. 6): in the expression for KF, the exponent for Ions should be 0.5 (or 1/2) and not 1.5.
30th page (page nr. 7): “Every constant are corrected by the hydrostatic pressure” should read “All the constants are corrected for the effect of hydrostatic pressure”

Guy Munhoven
Liège, 9th October 2020

Implementation and assessment of a carbonate system model (Eco3M-CarbOx v1.1) in a highly-dynamic Mediterranean coastal site (Bay of Marseille, France).

Katixa Lajaunie-Salla[1], Frédéric Diaz[1], Cathy Wimart-Rousseau[1], Thibaut Wagener[1], Dominique Lefèvre[1], Christophe Yohia[2], Irène Xueref-Remy[3], Brian Nathan[3], Alexandre Armengaud[4], Christel Pinazo[1]

[1]Aix Marseille Univ., Université de Toulon, CNRS, IRD, MIO, UM 110, 13288, Marseille, France
[2]Aix Marseille Univ., CNRS, IRD, OSU Institut Pythéas, 13288, Marseille, France

[3]Aix Marseille Univ., Université d'Avignon, CNRS, IRD, IMBE, Marseille, France
[4]AtmoSud : Observatoire de la qualité de l'air en région Sud Provence Alpes Côte d'Azur, le Noilly Paradis, 146 ~~Rue~~rue Paradis, 13294 Marseille, Cedex 06, France

Correspondance to : Katixa Lajaunie-Salla (katixa.lajaunie~~-salla@mio.osupytheas.fr~~@gmail.com), Frédéric Diaz (frederic.diaz@univ-amu.fr)

Abstract. A carbonate chemistry balance module was implemented into a biogeochemical model of the planktonic food web. The model, named Eco3M-CarbOx includes 22 state variables that are dispatched into 5 compartments: phytoplankton, heterotrophic bacteria, detrital particulate organic matter, labile dissolved organic and inorganic matter. This model is applied to and evaluated in the Bay of Marseille (BoM, France) that is a coastal zone impacted by the urbanized and industrialized Aix-Marseille Metropolis, and subject to significant increases in anthropogenic emissions of CO_2.

The model was evaluated over the year 2017 ~~that is a period~~ for which *in situ* data of carbonate system are available in the study site. The biogeochemical state variables of the model only change with time, to represent the time evolution of a sea surface water cell in response to the implemented realistic forcing conditions. The model correctly simulates the values ranges and seasonal dynamics of most of variables of carbonate system except ~~Total Alkalinity.~~for the total alkalinity. Several numerical experiments were ~~also~~ conducted to test the response of carbonate system to (i) a seawater temperature increase, (ii) wind events, (iii) Rhône River plume ~~intrusion~~intrusions and (iv) levels of atmospheric CO_2 contents. This set of numerical experiments shows that the Eco3M-CarbOx model provides expected responses in the alteration of the marine carbonate balance regarding each of the considered perturbation. When the seawater temperature changes quickly, the behaviour of the BoM waters alters within a few days from a source of CO_2 to the atmosphere to a sink into the ocean. Moreover, the higher the wind speed is, the higher the air-sea CO_2 gas exchange fluxes are. The river intrusions with nitrate ~~and alkalinity~~ supplies lead to a decrease in the pCO_2 value, favouring the conditions of a sink for atmospheric CO_2 into the BoM. A scenario of high atmospheric concentrations of CO_2 also favours the conditions of a sink for atmospheric CO_2 into the waters of the BoM. Thus the model results suggest that external ~~forcing~~forcings have an important impact on the carbonate equilibrium in this coastal area.

Mis en forme

Mis en forme : Centré

1. Introduction

Current climate change mostly originates from the carbon dioxide (CO_2) increase in the atmosphere at a high annual rate (+2.63 ppm from May 2018 to May 2019, https://www.esrl.noaa.gov/gmd/ccgg/trends/global.html). This atmospheric CO_2 increase impacts the carbonate chemistry equilibrium of the oceanic water column (Allen et al., 2009; Matthews et al., 2009). Oceans are known to act as a sink for anthropogenic CO_2, *i.e.* 30% of emissions, which leads to a marine acidification (Gruber et al., 2019; Orr et al., 2005; Le Quéré et al., 2018).

CO_2 is a key molecule in the biogeochemical functioning of the marine ecosystem. Photo-autotrophic organisms, mainly phytoplankton and macro-algae, fix this gas through photosynthesis in the euphotic zone and, in turn, produce organic matter and dissolved oxygen. Heterotrophic organisms, mainly heterotrophic protists and metazoans consume organic matter and dissolved oxygen by aerobic respiration and, in turn, produce CO_2. In the Ocean, the main processes regulating CO_2 exchanges between the atmosphere and sea are the solubility pump and the biological pump at different time-scales. Overall, the thermohaline gradients drive the solubility pump, while the metabolic processes of gross primary production and respiration set the intensity of the biological pump (Raven and Falkowski, 1999).

The coastal zones, despite their small surface area and volume compared to those of the open ocean, have a large influence upon carbon dynamics and represent 14 to 30% of the oceanic primary production (Gattuso et al., 1998). At the interface between open-ocean and continents, these zones receive large inputs of nutrients and organic matter from rivers, groundwater discharge, and from atmospheric depositions (Cloern et al., 2014; Gattuso et al., 1998). ~~On the coastline, coastal areas~~On coasts, shorelines are subject to an increasing density of population and associated urbanization (Small and Nicholls, 2003). This rapid alteration of ~~the coastline~~shorelines all over the world accelerates the emissions of greenhouses gases near the coastal ocean, and it also involves large discharges of material into the seawater by wastewater runoff and/or rivers (Cloern, 2001). These anthropogenic forcing alter the biogeochemical functioning of these zones and could lead to a growing eutrophication (Cloern, 2001). Moreover, these forcing could affect the carbonate chemistry dynamics and amplify or attenuate the acidification in coastal zones. This alteration of the marine environment may provoke further changes in the structure of the plankton community, including *in fine* consequences on the populations with high trophic levels, such as teleosts (Esbaugh et al., 2012). At the global scale, coastal zones are considered to be a significant sink for atmospheric CO_2, with an estimated flux converging to 0.2 PgC y^{-1} (Roobaert et al., 2019). However, some studies highlight that the status of these areas as a net sink or source still remains uncertain due to the complexity of the interactions between biological and physical processes, and also due to the lack of *in situ* measurements (Borges and Abril, 2011; Chen et al., 2013; Chen and Borges, 2009). Moreover, the capacity for coastal zones to absorb atmospheric CO_2 resulting from the increasing human pressure also remains poorly known. There are few works which highlight, under future atmospheric CO_2 levels, ~~that shallow seas~~whether coastal zones will become a net sink or a reduced source of CO_2 (Andersson and Mackenzie, 2012; Cai, 2011).

The current increase in the atmospheric CO_2 partial pressure (pCO_2) ~~in the surface ocean~~ is slowly shifting the marine carbonate chemistry equilibrium towards increases in the seawater pCO_2 and bicarbonate ions (HCO_3^-) and decreases in *p*H and carbonate ions (CO_3^{2-}) (Hoegh-Guldberg et al., 2018). These trends were already described in several coastal and open-ocean locations worldwide (Cai et al., 2011). In a coastal Northwestern Mediterranean site, a 10-year time-series of *in situ* measurements highlights a trend of *p*H decrease and pCO_2 increase (Kapsenberg et al., 2017). Low *p*H values can inhibit the ability of many marine organisms to form the calcium carbonate ($CaCO_3$) used in the making of skeletons and shells (Gattuso et al., 2015). In an extreme case, this shift may promote dissolution of $CaCO_3$ because the water will become under-saturated with respect to $CaCO_3$ minerals (Doney et al., 2009).

The present study is dedicated to the implementation of a carbonate system module into a preexisting biogeochemical model of planktonic food web. This new model, named Eco3M-CarbOx (v1.1) is then evaluated in a highly-dynamic

Mis en forme : Centré

coastal site, *i.e.* Bay of Marseille (BoM) in the Northwestern Mediterranean Sea. This evaluation is performed on the seasonal dynamics of biogeochemical and carbonate modeled variables against that of the corresponding *in situ* data available over the year 2017. This study is extended by a fine analysis of the variability of the marine carbonate system (stocks, fluxes) in relation to physical (*e.g.* wind events, river intrusions, temperature increases, changes in the atmospheric pCO_2 levels) and biogeochemical processes (gross primary production (GPP) and respiration (R)) in the study site. The BoM is suitable to this kind of study because this coastal area is subject to high emissions of atmospheric CO_2 from the nearby urban area, and it also receives effluents from the Aix-Marseille metropolis. In addition, strong wind events (Mistral) regularly occur, which could lead to (i) strong latent heat losses at the surface (Herrmann et al., 2011) and upwelling along the coast with a common consequence of cooling effect and (ii) ~~Rhone~~Rhône River plume intrusion under specific wind conditions (Fraysse et al., 2013, 2014). In this regional context, many anthropogenic forcing can interact with the dynamics of the carbonate systems. Natural determinants of the composition of the marine planktonic community can also play a crucial role in these dynamics.

2. Materials & Methods

2.1 Numerical model description

The Eco3M-CarbOx biogeochemical model was developed to represent the dynamics of the seawater carbonate system and plankton food web in the BoM. The model was implemented using the Eco3M (Ecological Mechanistic and Modular Modelling) platform (Baklouti et al., 2006). The model structure used is based on an existing model of the plankton ecosystem (Fraysse et al., 2013), including a description of Carbon (C), Nitrogen (N) and Phosphorus (P) marine biogeochemical cycles. The Eco3M-CarbOx model includes 22 prognostic state variables that are split into 5 compartments: phytoplankton, heterotrophic bacteria, detrital particulate organic matter, labile and semi-labile dissolved organic matter, nutrients (ammonia, nitrate and phosphate), dissolved oxygen, and carbonate system variables (Fig. 1). In this study, the state variables of the Eco3M-CarbOx model only change along time (*i.e.* usually termed "model 0D"), they are representative of the time evolution of a sea surface water cell but this biogeochemical model is not coupled with a hydrodynamic model.

The model presented in this study includes a set of new developments and improvements in the realism of the plankton web structure and process formulations compared to the model of Fraysse et al. (2013). In order to improve the representation of chlorophyll concentration in the Bay of Marseille the phytoplankton is divided in two groups: one with some ecological and physiological traits of the *Synechococcus* cyanobacteria, which is one of the major constitutive members of pico-autotrophs in Mediterranean Sea (Mella-Flores et al., 2011), and another with traits of large diatoms, which are generally observed during spring blooms at mid-latitudes (Margalef, 1978). For both of the phytoplankton, there is a diagnostic chlorophyll-a variable related to the phytoplankton C-biomass, the phytoplankton N-to-C ratio, and the limiting internal ratio f_Q^N (Faure et al., 2010; Smith and Tett, 2000; Tab. B2, Appendix B). The functional response of primary production was modified using another formulation of temperature limitation function which takes into account the optimal temperature of growth for each phytoplankton group. The exudation of phytoplankton was modified taking into account the intracellular phytoplankton ratio. For the uptake of matter by bacteria and the remineralization processes the dependence on intracellular bacteria ratio was modified. A temperature dependence of all biogeochemical processes was added to take into account the effects of rapid and strong variations of seawater temperature on plankton during episodes of upwelling for instance that are usually observed in the BoM. Also certain parameters in some formulations were modified owing to the alterations of some formulations. (Tabs. B4 & B5, Appendix B).

Mis en forme : Centré

Additionally, a carbonate system module was developed and three state variables were added: dissolved inorganic carbon (DIC), total alkalinity (TA) and the calcium carbonate ($CaCO_3$) implicitly representing calcifying organisms. The knowledge of DIC and TA allows the calculation of the pCO_2 and pH (total pH scale) diagnostic variables, necessary for resolving all the equations of the carbonate system. These equations use apparent equilibrium constants, which depend on temperature, pressure, and salinity (Dickson, 1990a, 1990b; Dickson and Riley, 1979; Lueker et al., 2000; Millero, 1995; Morris and Riley, 1966; Mucci, 1983; Riley, 1965; Riley and Tongudai, 1967; Uppström, 1974; Weiss, 1974). The details of the resolution of carbonate system module are given in the Appendix A. For this module three processes were also added: the precipitation and dissolution of calcium carbonate and the gas exchange of pCO_2 with the atmosphere. Based on the review of Middelburg (2019), it is considered that: (i) TA decreases by 2 moles for each mole of $CaCO_3$ precipitated, by 1 mole for each mole of ammonium nitrified, by 1 mole for each mole of ammonium assimilated by phytoplankton, and TA increases by 2 moles for each mole of $CaCO_3$ dissolved, and by 1 mole for each mole of organic matter mineralized by bacteria in ammonium (~~See~~Tab. B2, Appendix B ~~Tab. B2~~). (ii) DIC is consumed during the photosynthesis and calcification processes and is produced by respiration (of phytoplankton, zooplankton, and bacteria) and the $CaCO_3$ dissolution processes. Moreover, the dynamics of DIC are altered by the CO_2 exchanges with the atmosphere (Tab. B2, Appendix B). The air-sea CO_2 fluxes are calculated from the pCO_2 gradient across the air-sea interface and the gas transfer velocity (Tab. B3, Appendix B) estimated from the wind speed and using the parametrization of Wanninkhof (1992).

In the Eco3M-CarbOx model, zooplankton is considered as an implicit variable. However, a closure term based on the assumption that all of the matter grazed by the zooplankton and higher trophic levels returns as either organic or inorganic matter by excretion, egestion and mortality processes is taken into account (Fraysse et al., 2013). The model considers a "non-redfieldian" stoichiometry for phytoplankton and bacteria. All the biogeochemical model formulations, equations and associated parameters values are detailed in the Appendix B.

2.2 Study area

The BoM is located in the eastern part of the Gulf of Lions, in the Northwestern Mediterranean Sea (Fig. 2). The city of Marseille, located on the coast of the BoM, is the second largest city of France, with a population of *ca*. 1 million. The ~~Rhone~~Rhône River, which flows into the Gulf of Lions, is the greatest source of freshwater and nutrients for the Mediterranean Sea, with a river mean flow of 1800 $m^3 s^{-1}$ (Pont et al., 2002). Several studies highlight the eastward intrusion events from the ~~Rhone~~Rhône River plume in the BoM under East and South-easterly wind conditions, which favor biological productivity (Fraysse et al., 2014; Gatti et al., 2006; Para et al., 2010). The biogeochemistry of the BoM is complex and highly driven by hydrodynamics. For example, North-Northwesterly winds induce upwelling events which bring upward cold and nutrient-rich waters (Fraysse et al., 2013). Moreover, the oligotrophic Northern Current occasionally intrudes into the BoM (Petrenko, 2003; Ross et al., 2016).

Despite the presence of several marine protected areas around the BoM (the Regional Park of Camargue, the Marine protected area Côte Bleue and the National Park of Calanques), it is strongly impacted by diverse anthropogenic forcing, because industrialized and urbanized areas are located all along the coast. From the land, the BoM receives nutrients and organic matter from the urban area of the Aix-Marseille metropolis (Millet et al., 2018), the industrialized area of Fos-sur-Mer (one of the biggest oil-based industry areas in Europe), and the Berre Lagoon, which is eutrophized (Gouze et al., 2008; Fig. 2C). From the atmosphere, the BoM is subject to fine particles deposition and greenhouse gas emissions (including CO_2) from the nearby urban area, and it also receives effluents from the Aix-Marseille metropolis.

2.3 Dataset

Mis en forme : Centré

The modelled variables of the carbonate system (DIC, TA, *p*H and pCO_2) and chlorophyll-a are hereafter compared to observations collected at the SOLEMIO station (Figs. 2C & 3), which is a component of the French national monitoring network (Service d'Observation en Milieu Littoral - SOMLIT, http://somlit.epoc.u-bordeaux1.fr/fr/). Major biogeochemical parameters have been recorded since 1994. Carbonate chemistry variables (*p*H, pCO_2, DIC and TA) have been available since 2016, every two weeks.

2.4 Design of numerical experiments

In the present work, the Eco3M-CarbOx model was run for the whole year of 2017. This year was chosen because *in situ* data of carbonate systems (DIC, TA, *p*H and pCO_2) are available for the whole year at the SOLEMIO station (Fig. 2C). The biogeochemical variables were initialized using *in situ* data from winter conditions (Tab. B1, Appendix B). The model was forced by time-series of sea surface temperature and salinity, wind (at 10 m), light, and atmospheric CO_2 concentrations. The sea temperature time-series is from *in situ* hourly data recorded at the Planier station (Fig. 2C). For salinity, hourly *in situ* data from the SOLEMIO station and from the CARRY buoy were used (Fig. 2C). Wind and light hourly time-series were extracted from the WRF meteorological model at the SOLEMIO station (Yohia, 2017). Finally, we used hourly atmospheric CO_2 values from *in situ* measurements recorded at the *Cinq Avenues* station (CAV station, Fig. 2B) by the AtmoSud Regional Atmospheric Survey Network, France (https://www.atmosud.org). This simulation is the reference simulation (noted S0). As highlighted previously, ~~Rhone~~Rhône River plume intrusions (due to wind-specific conditions) have an impact on the dynamics of primary production (Fraysse et al., 2014; Ross et al., 2016) and then on the seawater ~~CO_2 concentrations.~~carbonate system. Moreover, the seawater temperature and atmospheric CO_2 variations control the seawater CO_2 dynamics *via* the solubility equilibrium and gas exchange with the atmosphere (Middelburg, 2019). In order to quantify the impact of different forcing, several simulations (hereafter noted S), which are summarized in Table 1, were conducted:

- Impact of seawater temperature increase, S1: the forcing time-series of *in situ* temperatures was shifted by +1.5°C (Cocco et al., 2013).
- Impact of wind events: a first simulation S2 was run with a constant wind intensity of 7 m s^{-1} (2017 annual average wind speed) throughout the year and a second one (S3) with two three-day periods of strong wind speed (20 m s^{-1}) representative of short bursts of Mistral (data not shown) starting on May 15th and August 15th, and a constant value of 7 m s^{-1} the rest of the year.
- Impact of ~~Rhone~~nutrient supply (nitrate) during a Rhône River plume intrusion (~~a salinity~~S4). A threshold of 37 has been chosen to identify the presence of low-salinity waters from the ~~Rhone~~Rhône River plume~~):~~
  - ~~Nitrate inputs were simulated during~~ in the ~~river plume intrusions (S4):~~forcing file of salinity. Here, the ~~level~~contents of nitrate supplied by the river depends on the salinity ~~level~~. A relationship between these two variables was then established ~~using NO_3 and salinity data at~~for the SOLEMIO point from the MARS3D-RHOMA coupled physical and biogeochemical model (Fraysse et al., 2013; Pairaud et al., 2011)~~, which~~. This relationship has already been used successfully to reproduce realistic observed conditions in the studies of Fraysse et al. (2014) and Ross et al. (2016): $NO_{3intrusion}$ (mmol m^{-3}) = -1.~~7~~70×S + 65.
  - ~~TA inputs were simulated during river plume intrusions (S5): the level of TA supply by the river depends on the salinity. A relationship was established using *in situ* data from the SOLEMIO station during river intrusion: $TA_{intrusion}$ (µmol kg^{-1}) = -21.0×S + 3400.~~
- Non-urban atmospheric CO_2 concentrations (~~S6~~S5): this simulation takes into account the forcing of atmospheric CO_2 values measured at the *Observatoire de Haute Provence* station (OHP, Fig. 2B) located outside of the Aix-

Mis en forme : Couleur de police : Couleur personnalisée(RVB(35;31;32))

Mis en forme : Retrait : Gauche : 0 cm, Suspendu : 0,5 cm, Hiérarchisation + Niveau : 1 + Style de numérotation : Puce + Alignement : 1,26 cm + Retrait : 1,9 cm

Mis en forme : Centré

Marseille metropolis from the ICOS National Network, France (http://www.obs-hp.fr/ICOS/Plaquette-ICOS-201407_lite.pdf).

In this work, we calculated the daily mean values of state variables, ~~the~~ statistical parameters and mean fluxes of modeled processes throughout the year and over two main hydrological periods: the stratified and mixed water column periods. The stratified water column (SWC) is defined with a temperature difference between the surface and bottom of more than 0.5°C (Monterey and Levitus, 1997). For the simulated year (2017), the SWC period lasts from May 10th to October 20th. The mixed water column (MWC) period corresponds to the rest of the year.

3. Results

3.1 Model skills

Following the recommendations of Rykiel (1996), three criteria were considered to evaluate the performance of our model:

- Does the model reproduce the timing of the observed variations of carbonate system at the seasonal time scale?
- Does the model reproduce the observed pCO_2 and pH ranges at the seasonal time scale?
- Analysis of the Willmott Skill Score (WSS): this index is an objective measurement of the degree of agreement between the modeled results and the observed data. A correct representation of observations by the model is achieved when this index is higher than 0.70 (Willmott, 1982).

Over most of the studied period, the model simulates lower chlorophyll-a concentrations than the *in situ* observations, especially during the MWC period (Fig. 3A). Two maxima of chlorophyll-a concentrations are observed *in situ:* the first one at *ca*. 1.71 mg m^{-3} in March and the second one at *ca*. 0.68 mg m^{-3} in May. They are both linked to ~~Rhone~~Rhône River plume intrusions. Several *in situ* maxima between 0.50 and 0.70 mg m^{-3} are observed between March and April (at the end of the MWC period), and they signaled the spring bloom event (Tab. 2 & Fig. 3A). The biogeochemical model quantitatively reproduces the spring bloom observed at the end of the MWC period (Fig. 3A) with a maximum value of *ca.* 0.69 mg m^{-3}. The model does not catch the two aforementioned maxima of chlorophyll, and it contains a low WSS and a strong bias (0.37 and +0.22 mg m^{-3}, respectively - Tab. 2).

On the whole, the seasonal variations of the seawater pCO_2 are correctly simulated by the biogeochemical model (Fig. 3B), even if the values are rather overestimated during the MWC period. From January to February, the model reproduces the slight decrease in the observed pCO_2 and from February to March the increase in pCO_2 even if the latter modelled remains smaller. In mid-April, during the simulated spring bloom period, the observed drop in pCO_2 and increase in pH are also spotted in the model (Fig. 3B & 3C). The model especially succeeds in reproducing the observed increase in relation to high temperatures during the SWC period. The reduction of the CO_2 solubility due to thermal effects mostly explains the increase in pCO_2 during the SWC period. The strong standard deviation of modeled values during the SWC period can be explained by the rapid changes in temperature probably due to upwelling usually occurring at this time of the year (Millot, 1990). The range of modeled pCO_2 values (345 - 503 µatm) encompasses the range of observed values (358 - 471 µatm; Tab. 2). The statistical analysis provides a mean bias of +23 µatm, and a WSS of 0.69 (Tab. 2).

The seasonal dynamic of pH is mostly reproduced by the model, and in particular, the decrease during the SWC period (Fig. 3C). However, the modelled pH is generally underestimated throughout the year, except during the SWC period, with a mean bias of -0.015 (Tab. 2). The seasonal range is captured by the model with a minimum value during the

Mis en forme : Centré

SWC period (7.994 *vs.* 8.014 for observations; Tab.2) and a maximum one during the MWC period (8.137 *vs.* 8.114 for observations; Tab.2). The statistical analysis highlights an index of agreement between the *in situ* data and the model outputs higher than 0.70 (Tab. 2).

The seasonal variations of DIC show the highest values during the MWC period and a decrease (resp. increase) during the beginning (resp. the end) of the SWC period (Fig. 3D). The lowest values are observed during September. The Eco3M-CarbOx model closely matches the seasonal dynamic by reproducing the range of extreme observed values (Tab. 2). The mean bias is also small (-8.48 µmol kg^{-1}, Tab. 2). More than 70% (0.73, Tab. 2) of modeled DIC concentrations are in statistical agreement with the corresponding observations.

The seasonal cycle of measured TA does not show a clear pattern (Fig. 3E). Large variations of values ranging between 2561 and 2624 µmol kg^{-1} (Tab. 2) are observed, whatever the hydrological season is that is considered. The biogeochemical model provides almost constant values around 2570 µmol kg^{-1} all along the year, which is lower than *in situ* data. With a low WSS index of agreement and a large mean bias (Tab. 2), the model is not able to confidently reproduce the observed variations of TA (Fig. 3E & Tab. 2).

3.2 Carbon fluxes and budgets

For the year 2017, the values of temperature vary between 13.3°C and 25.9°C (Fig. 4A). The DIC variations closely match those of temperature (correlation coef. -0.75). For example, the spring increase in temperature leads to a decrease in DIC concentrations (Figs. 4A & 4C), and the minimum values are reached at the end of SWC period. Over the simulated period, the air-sea CO_2 fluxes (F_{aera}) vary between -14 and 17 mmol m^{-3} d^{-1}, with a weakly positive annual budget of +6 mmol m^{-3} y^{-1} (or +0.017 mmol m^{-3} d^{-1}, Tab. 3). Then, the BoM waters would act as a net source of CO_2 to the atmosphere on an annual basis. However, on a seasonal basis, the BoM waters would change from a net sink during the MWC period (F_{aera} <0; Tab. 3) to a net source during the SWC one (F_{aera} >0; Tab. 3).

On an annual basis, the gross primary production (GPP) and total respiration (R) are balanced, leading to a null average net ecosystem production (NEP, NEP=GPP-R) (Fig. 4F & Tab. 3). The intensity of autotroph respiration (R_a) is lower than that of primary production (annual mean of 0.065 *vs*. -0.413 mmol m^{-3} d^{-1}, respectively - Tab. 3). While the zooplankton and bacterial respiration account for an average of 0.348 mmol m^{-3} d^{-1} (Tab. 3). On a seasonal basis, the model highlights an ecosystem dominated by autotrophy during the MWC period (NEP>0; Tab. 3) and heterotrophy during the SWC period with higher fluxes values (NEP<0; Tab. 3). The biogeochemical fluxes show the strongest variations along the SWC period, following those of temperature (Fig. 4F). The maximum GPP occurs in April and is correlated with the maximum chlorophyll concentration. At this time, the ecosystem is autotroph (NEP>0; Figs. 4B & 4F), and is a net sink for atmospheric CO_2, which explains the DIC and seawater pCO_2 decreases during the bloom period (Figs. 4C, 4D & 4E)

When looking in details at the temperature and salinity 2017 time-series (Fig. 4A), several crucial events can be seen occurring, including freshwater intrusions (*e.g.* ~~15~~ March 15th and ~~6~~ May 6th) into the BoM and large variations of temperature in relation with upwelling events or latent heat losses due to wind bursts. The largest freshwater intrusion from the ~~Rhone~~Rhône River plume occurs in mid-March, with a minimum observed salinity of *ca*. 32.5 at the SOLEMIO station (Fig. 4A). During this event, the seawater pCO_2 decreases and *p*H increases concomitantly (Figs. 4C & 4D). Then, seawater appears to be temporarily under-saturated in CO_2 and the BoM waters thus acts as a sink for atmospheric CO_2 at the time of intrusion (Fig. 4E).

During the SWC period, upwelling events quickly cool the surface seawater. In two days, from July 25th to 27th, the water temperature drops from 24.7°C to 16.9°C (Fig. 4G). The decrease in temperature corresponds to the increase in DIC concentrations (Fig. 4I). Concomitantly, the values of seawater pCO_2 decrease from 497 to 352 µatm and *p*H

Mis en forme : Centré

increase from 7.99 to 8.12 (Figs. 4I & 4J). This event quickly changes the BoM waters from a source to a sink for atmospheric CO_2 (from +17 to -14 mmol m^{-3} d^{-1}, Fig. 4K), and also from a net heterotroph to a net autotroph ecosystem (Fig. 4L).

3.3 Impact of external forcing on the dynamics of carbonate system

3.3.1 Temperature increase

Here we compare the reference simulation S0 with the S1 simulation (seawater temperature elevation of 1.5°C - Fig. 5). During the year, there are few changes on the carbonate system variables such as the pCO_2 and pH (data not shown). The main alterations occur during the blooms of phytoplankton. The simulated bloom of phytoplankton occurs later, at beginning of May, for both diatoms and picophytoplankton, with a maximum value of chlorophyll at1.4 and 0.4 mg m^{-3}, respectively (Figs. 5A & 5F).

As both the limitations due to light and nutrients remain about the same during the simulations S0 and S1, this counterintuitive occurrence of bloom relative to changes in temperature is mainly explained by the temperature limiting function, which depends on the optimal temperature of growth (T_{opt}). For the picophytoplankton, from January to April, the increase of 1.5°C drastically reduces the limitation by temperature (Fig. 5C), because the temperature is closer to the optimal temperature (T_{opt}=16°C, Tab. A4) during S1 than S0. In the S0 simulation, the temperature reaches T_{opt} *ca.* April 15th and it induces the bloom, while at the same time in S1 the temperature moves slightly away from T_{opt} and it does not enable the triggering of a bloom. At the time of the bloom in S1, the opposite configuration occurs. In S0, the ambient temperature is again far from T_{opt}, explaining the absence of bloom, while in the S1 the ambient temperature is closer to T_{opt} enabling the occurrence of bloom. The picophytoplankton bloom then occurs later in the warm simulation S1 than in the reference simulation S0 (Fig. 5A). The duration and termination of bloom is controlled both by the nutrients availability and the temperature (Figs. 5C & 5D). Inversely, from January to April, the diatoms' growth limitation by temperature is strengthened in the warm simulation S1 (Fig. 5H), because the resulting ambient temperature is further from the optimum temperature (T_{opt}=13°C, Tab. A4) than that in the reference simulation S0. This induces a slower growth of diatoms and a delay of the maximum concentration (Fig. 5F). Afterwards the photosynthesis is mainly limited by temperature (Fig. 5H).

The ecosystem is net autotroph at the time of blooms whatever the simulation considered (NEP>0; Fig. 5E) and the quantity of DIC (not shown) fixed through autotroph processes is larger than that released by heterotroph processes. During the short period of bloom, the seawater pCO_2 decreases, leading to some negative air-sea fluxes (*i.e.* an oceanic sink for atmospheric CO_2). In the warm simulation, the later occurrence of bloom enables the period of the spring sink to extend by *ca*. three weeks over May relative to the reference simulation (Fig. 5J).

3.3.2 Wind speed

The Bay of Marseille is periodically under the influence of strong wind events (Millot, 1990). Here we compare two simulations: one with a constant wind value (S2) and the other one with two wind events that occur in May and August (S3) (Figs. 6A & D). The result of this numerical experiment shows that the stronger the wind speed is, the higher the air-sea fluxes are, mainly owing to the increase in gas transfer velocity. Depending on the gradient of CO_2 between seawater and the atmosphere, strong wind speeds will favor either the emission or uptake of CO_2 (Figs. 6B & E). In May, with the air-sea CO_2 flux being positive, the outgassing of CO_2 to the atmosphere is enhanced leading to a decrease in seawater pCO_2 (Fig. 6C). On the contrary, in August the oceanic sink of atmospheric CO_2 is amplified which leads to an increase in the seawater pCO_2 value (Fig. 6F).

Mis en forme : Centré

3.3.3 Supply in nitrate ~~and alkalinity~~ by river inputs

According to the model results (Fig. 7), the occasional inputs of nitrate (S4) that are linked to ~~Rhone~~Rhône River plume intrusions favor primary production and they led to increased chlorophyll concentrations (Figs. 7B & 7C) five times during the SWC period. These blooms, as seen previously, lead to a decrease (resp. increase) in the seawater pCO_2 (resp. *p*H) (Figs. 7E & 7F). It can be noted that with the strongest river supply at mid-March (Figs. 7A & 7B) the occurrence of the spring bloom is earlier (Fig. 7C) than that occurring in the reference simulation (S0). The time lag between river nutrient supply and bloom is due to the temperature limitation (Fig. 4C). During blooms occurring within the SWC period following intrusions, the DIC concentrations are generally lower than those of the reference simulation, as in the case of the bloom of mid-May (decrease by *ca*. 15 µmol kg^{-1}, Fig. 7J), due to the autotroph processes dominating the heterotroph ones. In turn, the seawater pCO_2 drops by *ca*. 30 µatm (Fig. 7K) and *p*H increases by *ca*. 0.030 (Fig. 7L). Nitrate inputs, favoring primary production, reduce the source of CO_2 to the atmosphere ~~or~~and intensify the sink of atmospheric CO_2 into the waters of BoM (~~Fig~~Figs. 7E & 7K).

~~The supply of alkalinity during the Rhone River plume intrusions (Fig. 8A) significantly increases the DIC concentrations (*ca*. +50 µmol kg^{-1}, Figs. 8B & 8F), in every hydrological period considered. During the strongest freshwater input at mid-March, the sharp TA increase by *ca*. +150 µmol kg^{-1} (Fig. 8E) leads to a large pCO_2 drop by *ca*. 92 µatm and a *p*H increase by 0.13 (Figs. 8G & 8H). The air-sea gradient of pCO_2 increases at mid-March, favoring sink conditions for atmospheric CO_2 into the waters of the BoM (Fig. 8G).~~

3.3.4 Urban air CO_2 concentrations

The Aix-Marseille metropolis is strongly subject to urban emissions to the atmosphere (Xueref-Remy et al., 2018a). The seasonal variability of atmospheric CO_2 concentrations at the urban site (CAV station, Fig. 2) is much higher than that observed in a non-urban area (OHP station, Fig. 2), especially during the MWC period (Fig. ~~9A~~8A): CO_2 concentrations vary between 379 and 547 µatm at the CAV station and between 381 and 429 µatm at the OHP station. Moreover, in winter the atmospheric pCO_2 is higher in the urban area than non-urban area, whereas in summer those of both areas are quite close. These differences in the seasonal pattern and between areas are usually explained by (i) the thinner atmospheric boundary layer, (ii) the decreased fixation of CO_2 by terrestrial vegetation, and (iii) the greater influence of anthropogenic activities by emissions from heating (Xueref-Remy et al., 2018b). Forcing the model by atmospheric pCO_2 values from urban or non-urban site can lead to significant differences in the values of the seawater pCO_2 during the MWC period especially. The air-sea gradient of pCO_2 is higher when using a forcing derived from the CO_2 concentrations originating from an urban area than from non-urban area, which strengthens the sink of atmospheric CO_2 into the waters of BoM. The seawater pCO_2 is then lower with non-urban area pressure (~~S6~~S5) than with urban area pressure (S0), because of lower CO_2 solubility in the BoM (Fig. ~~9B~~8B).

4. Discussion

4.1 Model performance

The evaluation of model skill *vs*. *in situ* data highlights that the modeled *p*H, pCO_2, DIC are in acceptable agreement with observations (Fig. 3). The seasonal variations observed for the different variables are captured by the model, including for example the seasonal decrease in DIC and *p*H during the SWC period, in relation to the increase in pCO_2, and the inverse scenario during the MWC period. The chlorophyll content variability is not well reproduced, especially during spring (Fig. 3A), even taking into account the nitrate supply from the ~~Rhone~~Rhône River plume intrusion (Fig. 7C). This is due to the multiple origins of chlorophyll, organic matter, and nutrients in the BoM that are not accounted

Mis en forme : Barré

Mis en forme : Centré

for in the Eco3M-CarbOx model: autochthonous marine production, and allochthonous origins from the ~~Rhone~~Rhône and Huveaune River plumes (Fraysse et al., 2013). The observed variations and levels of TA are not correctly simulated by the model (Fig. ~~3F), even taking into account the supply of TA coming from the Rhone River plume (Fig. 8). The formulation used in this study for TA inputs from rivers needs to be refined and compared with other works (Gemayel et al., 2015; Schneider et al., 2007).~~3F). The study of Soetaert et al. (2007) highlights that the main variations of TA in the marine coastal zones are linked to freshwater supplies and marine sediments. The present study does not take into account the inputs of TA from the Rhône River and the water-sediment interface, and it may explain why the TA variable is not correctly predicted by our model.

4.2 Contribution of physical and biogeochemical processes to the variability of carbonate system

The contribution of each biogeochemical process to the DIC variability can be assessed using the presented model: the aeration process contributes to 78% of the DIC variations and biogeochemical processes together to 22% (Tab. 3). As mentioned by Wimart-Rousseau et al. (2020), the model suggests that the seawater pCO_2 variations and associated fluxes would be mostly driven by the seawater temperature dynamics. Moreover, the seasonal variations of the air-sea CO_2 flux are in agreement with some previous field studies (De Carlo et al., 2013; Wimart-Rousseau et al., 2020), which measured a weak oceanic sink for atmospheric CO_2 during winter and a weak source to the atmosphere during summer.

The model results reveal that temperature would play a crucial role in controlling two counterbalanced processes: (1) the carbonate system equilibrium and (2) the phytoplankton growth. The increase in temperature during SWC leads to a higher pCO_2 in seawater due to the decrease in the CO_2 solubility (Middelburg, 2019) and, at the same time, the fixation of DIC by phytoplankton is favored, leading to a decrease in the pCO_2 level. The imbalance between the latter two processes leads to a change in the ecosystem status (autotrophic or heterotrophic) and the corresponding behavior as a sink or source to the atmosphere. In case of a 1.5°C rise over the whole year, the temperature variation has a very small impact on the carbonate system dynamics. However, it favors the autotrophic processes and strengthens the oceanic sink of atmospheric CO_2 during the bloom of phytoplankton (Figs. 5E & 5J).

4.3 Contribution of the external forcing to the variability of carbonate system

In line with several previous works on the Northwestern Mediterranean Sea (De Carlo et al., 2013; Copin-Montégut et al., 2004; Wimart-Rousseau et al., 2020), the model also suggests that the status of the Bay of Marseille regarding sink or source for CO_2 could change at high temporal frequency (*i.e.* hours to days). Bursts of North, Northwestern winds, lead to sudden and sharp decreases in seawater temperature (<2 days, Fig. 4G) either directly by latent heat loss through evaporation at the surface (Herrmann et al., 2011) or indirectly by creating upwelling (Millot, 1990), with the consequences of decrease in the seawater pCO_2 values (Fig. 4J) and *in fine*, an alteration of the CO_2 air-sea fluxes. Model results suggest that the fast variations of temperature could lead to rapid changes of the sink *vs.* source status in this coastal zone (Fig. 4K). ~~Moreover, previous study on the BoM highlights that upwelling favors ephemeral blooms of phytoplankton by nutrient supplies up to euphotic layer (Fraysse et al., 2013) and would, in turn, contribute to the seawater pCO_2 decrease.~~Moreover, Fraysse et al. (2013) highlight that upwelling in the BoM favors ephemeral blooms of phytoplankton by nutrient supplies up to euphotic layer and would, in turn, contribute to the seawater pCO_2 decrease. North, and Northwestern winds through latent heat losses and/or upwelling events could then enhance the sink for atmospheric CO_2 due to the temperature drop and nutrients inputs. However, these results remain to be preliminary because in our experimental design only the cooling effect of upwelling on the carbonate balance is taken into account. But concomitantly, upwelling usually bring nutrients and DIC at the surface and these supplies could also perturb the

Mis en forme : Police :Non Italique

Mis en forme : Centré

balance of the carbonate system. A next coupling of the Eco3M-CarbOx model with a tridimensional hydrodynamic model would enable to certainly embrace the multiple effects of upwelling on the dynamics of the carbonate system in this area and refine the results presented in this study.

High wind speeds (>7 m s^{-1}) amplified considerably the gaseous exchange of CO_2 (De Carlo et al., 2013; Copin-Montégut et al., 2004; Wimart-Rousseau et al., 2020). The model highlights that a strong wind event of 3 days has a significant impact on the seawater pCO_2 values during a longer period of *ca.* 15 days (Fig. 6). A combination of high atmospheric pCO_2 value and high wind speed would then favor the sink for CO_2 into the waters of the BoM. The aeration process depends also on the choice of the formulation of the gas transfer velocity (k_{600}). In this study, the formulation of Wanninkhof (1992) is used and depends of the wind speed at 10 m above the water surface. However, the current velocity could favor the gas exchange and suspended matter concentration could limit the gas exchange (Abril et al., 2009; Upstill-Goddard, 2006; Zappa et al., 2003). Due to the important heterogeneity of physical and biogeochemical forcings in coastal zones, other factors that control the air-sea gas exchange should certainly be taken into account.

The simulation with intrusions of the ~~Rhone~~Rhône River plume shows that inputs of nitrate ~~and TA~~ cause a drop of seawater pCO_2 ~~duc~~owing to ~~some two concomitant effects:~~ nutrients supply ~~favors~~favoring the phytoplankton development ~~and TA inputs~~(Fig. 7). In this scenario, the oceanic sink of atmospheric CO_2 is enhanced. But rivers also supply TA (*e.g.* Gemayel et al., 2015; Schneider et al., 2007) and DIC (*e.g.* Sempéré et al., 2000) that shift the carbonate system equilibrium ~~leading to~~toward a pCO_2 decrease and a DIC increase (Middelburg, 2019) ~~(Figs. 7 & 8). The consequence is that the oceanic sink of CO_2 is enhanced. In fact, the experimental design on the Rhone River supply only considers the TA perturbation on the carbonate system but not that due to the DIC supply. To take into account the latter supply may further impact the DIC concentration when intrusions occur and it could sensibly modify the~~. Taking into account these further supplies may sensibly modify the modeled carbonate balance in the BoM. A next step to the present work will be to design more realistic numerical experiments to refine the results obtained in this preliminary study. The intrusions of ~~Rhone~~Rhône River plume also induce a salinity decrease of the BoM waters, which leads to drop the pCO_2 levels in the model. This drop of pCO_2 is due to the decrease in the CO_2 solubility when salinity decreases (Middelburg, 2019).

In the scenario of forcing the model by using urban atmospheric pCO_2 time-series, the air-sea gradient increases and then, it enhances the status of the BoM as a sink for atmospheric CO_2. As suggested by the *in situ* study of Wimart-Rousseau et al. (2020), the Eco3M-Carbox model highlights the crucial role of the coastal ocean in urbanized area, with an increase in atmospheric CO_2, the CO_2 uptake by the costal ocean may increase. This results is in line with studies of Andersson and Mackenzie (2004) and Cai (2011) that predict an increase in the intensity of CO_2 sink ~~in coastal areas due to high atmospheric CO_2 levels~~ and a potential threat to coastal marine biodiversity~~.~~ in coastal areas owing to high atmospheric CO_2 levels.

5. Conclusion

A marine carbonate chemistry module was implemented in the Eco3M-CarbOx biogeochemical model and evaluated against *in situ* data available in the Bay of Marseille (Northwestern Med. Sea) over the year 2017. The model correctly simulates the values ranges and seasonal dynamics of most of variables of the carbonate system except ~~Total Alkalinity~~for the total alkalinity. Several numerical experiments were also conducted to test the sensitivity of carbon balance to physical processes (temperature and salinity), biogeochemical processes (GPP and respiration processes) and external forcing (wind, river intrusion and atmospheric CO_2). This set of numerical experiments shows that the

Mis en forme : Centré

Eco3M-CarbOx model provides expected responses in the alteration of the marine carbonate balance regarding each of the considered perturbation.

On the whole, the model results suggest that the carbonate system is mainly driven by the seawater temperature dynamics. At a seasonal scale, the BoM marine waters appear to be a net sink of atmospheric CO_2 and a dominant autotroph ecosystem during the MWC period, and a net source of CO_2 to the atmosphere during the SWC period, which is mainly characterized by a dominance of heterotroph processes. However, the model results highlight that sharp seawater cooling observed within the SWC period and probably owing to upwelling events, ~~causes~~cause the CO_2 status of the BoM marine waters to change from a source to the atmosphere to a sink into the ocean within a few days. External forcing as the temperature increases leads to a delay in the bloom of phytoplankton. Strong wind events enhance the gas exchange of CO_2 with the atmosphere. A ~~Rhone~~Rhône River plume intrusion with input of nitrate ~~and alkalinity~~ favors pCO_2 decreases, and the sink of atmospheric CO_2 into the BoM waters is enhanced. The higher ~~air~~atmospheric pCO_2 values from the urban area intensify the oceanic sink of atmospheric CO_2.

The BoM biogeochemical functioning is mainly forced by wind-driven hydrodynamics (upwelling, downwelling), urban rivers, wastewater treatment plants, and atmospheric deposition (Fraysse et al., 2013). In addition, Northern Current and ~~Rhone~~Rhône River plume intrusions frequently occurred (Fraysse et al., 2014; Ross et al., 2016). Moreover, the BoM harbors the second bigger metropolis of France (Marseille) that is impacted by many harbor activities. The next step of this study will be to couple the Eco3M-CarbOx biogeochemical model to a 3D hydrodynamic model that will mirror the complexity of the BoM functioning. In this way, the contributions of hydrodynamic, atmospheric, anthropic, and biogeochemical processes to the DIC variability will be able to be determined with higher refinement and realism, and an overview of the air-sea CO_2 exchange could be made at the scale of the Bay of Marseille. The main results of our study could be transposed to other coastal sites that are also impacted by urban and anthropic pressures. Moreover, in this paper we highlighted that fast and strong variations of pCO_2 values occur, so thus it is essential to acquire more *in situ* values at high frequency (at least with an hourly resolution) to understand the rapid variations of the marine carbon system at these short spatial and temporal scales.

Mis en forme : Centré

Acknowledgements

We thank the National Service d'Observation en MILieu Littoral (SOMLIT) for its permission to use SOLEMIO data. We wish to thank the crewmembers of the R.V. 'Antedon II', operated by the DT-INSU, for making these samplings possible. We wish to acknowledge the team of the SAM platform (Service Atmosphère Mer) of MIO institute for their helping in field work. For the collection and analyses of the seawater sample, we thank Michel Lafont and Véronique Lagadec of the PACEM (Plateforme Analytique de Chimie des Environnenments Marins) platform of MIO institute and also the SNAPO-CO2 at LOCEAN, Paris. The SNAPO-CO2 service at LOCEAN is supported by CNRS-INSU and OSU Ecce-Terra.

We acknowledge the staff of the "Cluster de calcul intensif HPC" Platform of the OSU Institut Pythéas (Aix-Marseille Université, INSU-CNRS) for providing the computing facilities. We gratefully acknowledge Julien Lecubin from the Service Informatique de OSU Institut Pythéas (SIP) for their technical assistance. Moreover, we thank Camille Mazoyer and Claire Seceh for their contribution on the Eco3M-CarbOx model development.

Financial support

This study is part of the AMC project (Aix-Marseille Carbon Pilot Study, 2016-2019) funded and performed in the framework of the Labex OT-MED (ANR-11-LABEX-0061, part of the "Investissement d'Avenir" program through the A*MIDEX project ANR-11-IDEX-0001-02), funded by the French National Research Agency (ANR). The project leading to this publication has received funding from the European FEDER Fund under project 1166-39417.

Code availability

Eco3M is freely available under CeCILL license agreement (a French equivalent to the L-GPL license; http://cecill.info/licences/Licence_CeCILL_V1.1-US.html; last access: 10 February 2020). The Eco3M-CarbOx model is written in Fortran-90/95 and the plotting code is written in Matlab®. The exact version of the model used to produce the results presented in this paper is archived on Zenodo (DOI: 10.5281/zenodo.3757677) (last access: 24 August 2020). A short User Manual is given in the Appendix C of this study.

Mis en forme : Centré

References

Abril, G., Commarieu, M. V., Sottolichio, A., Bretel, P. and Guérin, F.: Turbidity limits gas exchange in a large macrotidal estuary, Estuar. Coast. Shelf Sci., 83, 342–348, doi:10.1016/j.ecss.2009.03.006, 2009.

Allen, M. R., Frame, D. J., Huntingford, C., Jones, C., Lowe, J. A., Meinshausen, M. and Meinshausen, N.: Warming caused by cumulative carbon emissions towards the trillionth tonne, Nature, 458, 1163–1166, doi:10.1038/nature08019, 2009.

Andersson, A. J. and Mackenzie, F. T.: Shallow-water oceans: a source or sink of atmospheric CO_2?, Front. Ecol. Environ., 2(7), 348–353, doi:10.1890/1540-9295, 2004.

Andersson, A. J. and Mackenzie, F. T.: Revisiting four scientific debates in ocean acidification research, Biogeosciences, 9(3), 893–905, doi:10.5194/bg-9-893-2012, 2012.

Auger, P. A., Diaz, F., Ulses, C., Estournel, C., Neveux, J., Joux, F., Pujo-Pay, M. and Naudin, J. J.: Functioning of the planktonic ecosystem on the Gulf of Lions shelf (NW Mediterranean) during spring and its impact on the carbon deposition: a field data and 3-D modelling combined approach, Biogeosciences, 8(11), 3231–3261, doi:10.5194/bg-8-3231-2011, 2011.

Baklouti, M., Faure, V, Pawlowski, L. and Sciandra, A.: Investigation and sensitivity analysis of a mechanistic phytoplankton model implemented in a new modular numerical tool (Eco3M) dedicated to biogeochemical modelling. Prog. Oceanogr., 71(1), 34-58, doi:10.1016/j.pocean.2006.05.003, 2006.

Borges, A. V and Abril, G.: Carbon ~~Dioxide~~dioxide and ~~Methane Dynamics~~methane dynamics in ~~Estuaries~~estuaries, in Treatise on Estuarine and Coastal Science, edited by E. Wolanski and D. McLusky, pp. 119–161, Academic Press, Waltham., 2011.

Le Borgne, R.: Zooplankton production in the eastern tropical Atlantic Ocean: Net growth efficiency and P:B in terms of carbon, nitrogen, and phosphorus, Limnol. Oceanogr., 27(4), 681–698, doi:10.4319/lo.1982.27.4.0681, 1982.

Le Borgne, R. and Rodier, M.: Net zooplankton and the biological pump: a comparison between the oligotrophic and mesotrophic equatorial Pacific, Deep Sea Res. Part II ~~Top. Stud. Oceanogr.,~~ 44(9), 2003–2023, doi:10.1016/S0967-0645(97)00034-9, 1997.

Cai, W.-J.: Estuarine and ~~Coastal Ocean Carbon Paradox~~coastal ocean carbon paradox: CO_2 ~~Sinks~~sinks or ~~Sites~~sites of ~~Terrestrial Carbon Incineration~~terrestrial carbon incineration?, Ann. Rev. Mar. Sci., 3(1), 123–145, doi:10.1146/annurev-marine-120709-142723, 2011.

Cai, W.-J., Hu, X., Huang, W.-J., Murrell, M. C., Lehrter, J. C., Lohrenz, S. E., Chou, W.-C., Zhai, W., Hollibaugh, J. T., Wang, Y., Zhao, P., Guo, X., Gundersen, K., Dai, M. and Gong, G.-C.: Acidification of subsurface coastal waters enhanced by eutrophication, Nat. Geosci., 4(11), 766–770, doi:10.1038/ngeo1297, 2011.

Campbell, R., Diaz, F., Hu, Z., Doglioli, A., Petrenko, A. and Dekeyser, I.: Nutrients and plankton spatial distributions induced by a coastal eddy in the Gulf of Lion. Insights from a numerical model, Prog. Oceanogr., 109, 47–69, doi:10.1016/j.pocean.2012.09.005, 2013.

De Carlo, E. H., Mousseau, L., Passafiume, O., Drupp, P. S. and Gattuso, J.-P.: Carbonate Chemistry and Air–Sea CO_2 Flux in a NW Mediterranean Bay Over a Four-Year Period: 2007–2011, Aquat. Geochemistry, 19(5–6), 399–442, doi:10.1007/s10498-013-9217-4, 2013.

Chen, C.-T. A. and Borges, A. V: Deep-Sea Research II Reconciling opposing views on carbon cycling in the coastal ocean~~:~~ : Continental shelves as sinks and near-shore ecosystems as sources of atmospheric CO_2, Deep Sea Res. II, 56, 578–590, doi:10.1016/j.dsr2.2009.01.001, 2009.

Chen, C.-T. A., Huang, T.-H., Chen, Y.-C., Bai, Y., He, X. and Kang, Y.: Air–sea exchanges of CO_2 in the world's coastal seas, Biogeosciences, 10(10), 6509–6544, doi:10.5194/bg-10-6509-2013, 2013.

Cloern, J. E.: Our evolving conceptual model of the coastal eutrophication problem, Mar. Ecol. Prog. Ser., 210, 223–253, doi:10.3354/meps210223, 2001.

Cloern, J. E., Foster, S. Q. and Kleckner, A. E.: Phytoplankton primary production in the world's estuarine-coastal ecosystems, Biogeosciences, 11, 2477–2501, doi:10.5194/bg-11-2477-2014, 2014.

Cocco, V., Joos, F., Steinacher, M., Frölicher, T. L., Bopp, L., Dunne, J., Gehlen, M., Heinze, C., Orr, J., Oschlies, A., Schneider, B., Segschneider, J. and Tjiputra, J.: Oxygen and indicators of stress for marine life in multi-model global warming projections, Biogeosciences, 10(3), 1849–1868, doi:10.5194/bg-10-1849-2013, 2013.

Copin-Montégut, C., Bégovic, M. and Merlivat, L.: Variability of the partial pressure of CO_2 on diel to annual time scales in the Northwestern Mediterranean Sea, Mar. Chem., 85(3), 169–189, doi:10.1016/j.marchem.2003.10.005, 2004.

Dickson, A. G.: Standard potential of the reaction: $AgCl_{(s)} + 12H_{2(g)} = Ag_{(s)} + HCl_{(aq)}$, and and the standard acidity constant of the ion HSO_4^- in synthetic sea water from 273.15 to 318.15 K, J. Chem. Thermodyn., 22(2), 113–127, doi:10.1016/0021-9614(90)90074-Z, 1990a.

Dickson, A. G.: Thermodynamics of the dissociation of boric acid in synthetic seawater from 273.15 to 318.15 K, Deep Sea Res~~. Part A. Oceanogr. Res. Pap~~., 37(5), 755–766, doi:10.1016/0198-0149(90)90004-F, 1990b.

Dickson, A. G. and Riley, J. P.: The estimation of acid dissociation constants in sea-water media from potentiometric titrations with strong base. II. The dissociation of phosphoric acid, Mar. Chem., 7(2), 101–109, doi:10.1016/0304-

Mis en forme : Centré

4203(79)90002-1, 1979.

Doney, S. C., Tilbrook, B., Roy, S., Metzl, N., Le Quéré, C., Hood, M., Feely, R. a. and Bakker, D.: Surface-ocean CO_2 variability and vulnerability, Deep Sea Res. Part II ~~Top. Stud. Oceanogr.~~, 56(8–10), 504–511, doi:10.1016/j.dsr2.2008.12.016, 2009.

Esbaugh, A. J., Heuer, R. and Grosell, M.: Impacts of ocean acidification on respiratory gas exchange and acid~~-~~–base balance in a marine teleost, Opsanus beta, J. Comp. Physiol. B, 182(7), 921–934, doi:10.1007/s00360-012-0668-5, 2012.

Faure, V., Pinazo, C., Torréton, J.-P. and Jacquet, S.: Modelling the spatial and temporal variability of the SW lagoon of New Caledonia I: A new biogeochemical model based on microbial loop recycling, Mar. Pollut. Bull., 61(7), 465–479, doi:10.1016/j.marpolbul.2010.06.041, 2010.

Fraysse, M., Pinazo, C., Faure, V., Fuchs, R., Lazzari, P., Raimbault, P. and Pairaud, I.: Development of a 3D ~~Coupled Physical-Biogeochemical Model~~coupled physical-biogeochemical model for the Marseille ~~Coastal Area~~coastal area (NW Mediterranean Sea): What ~~Complexity Is Required~~complexity is required in the Coastal Zone?, PLoS One, 8(12), 1–18, doi:10.1371/journal.pone.0080012, 2013.

Fraysse, M., Pairaud, I., Ross, O. N., Faure, V. and Pinazo, C.: Intrusion of ~~Rhone~~Rhône River diluted water into the Bay of Marseille: Generation processes and impacts on ecosystem functioning, J. Geophys. Res. Ocean., 119(10), 6535–6556, doi:10.1002/2014JC010022, 2014.

Fukuda, R., Ogawa, H., Nagata, T. and Koike, I.: Direct Determination of Carbon and Nitrogen Contents of Natural Bacterial Assemblages in Marine Environments, Appl. Environ. Microbiol., 64(9), 3352–3358 [online] Available from: https://aem.asm.org/content/64/9/3352, 1998.

Gatti, J., Petrenko, A., Devenon, J.-L., Leredde, Y. and Ulses, C.: The ~~Rhone~~Rhône river dilution zone present in the northeastern shelf of the Gulf of Lion in December 2003, Cont. Shelf Res., 26(15), 1794–1805, doi:10.1016/j.csr.2006.05.012, 2006.

Gattuso, J.-P., Frankignoulle, M. and Wollast, R.: Carbon and carbonate metabolism in coastal aquatic ecosystems, Annu. Rev. Ecol. Syst., 29(1), 405–34, doi:10.1146/annurev.ecolsys.29.1.405, 1998.

Gattuso, J.-P., Magnan, A., Bille, R., Cheung, W. W. L., Howes, E. L., Joos, F., Allemand, D., Bopp, L., Cooley, S. R., Eakin, C. M., Hoegh-Guldberg, O., Kelly, R. P., Portner, H.-O., Rogers, A. D., Baxter, J. M., Laffoley, D., Osborn, D., Rankovic, A., Rochette, J., Sumaila, U. R., Treyer, S. and Turley, C.: Contrasting futures for ocean and society from different anthropogenic CO_2 emissions scenarios, Science, 349(6243), pp.aac4722, doi:10.1126/science.aac4722, 2015.

Gehlen, M., Gangstø, R., Schneider, B., Bopp, L., Aumont, O. and Ethe, C.: The fate of pelagic $CaCO_3$ production in a high CO_2 ocean: a model study, Biogeosciences, 4(4), 505–519, doi:10.5194/bg-4-505-2007, 2007.

Gemayel, E., Hassoun, A. E. R., Benallal, M. A., Goyet, C., Rivaro, P., Abboud-Abi Saab, M., Krasakopoulou, E., Touratier, F. and Ziveri, P.: Climatological variations of total alkalinity and total dissolved inorganic carbon in the Mediterranean Sea surface waters, Earth Syst. Dyn., 6(2), 789–800, doi:10.5194/esd-6-789-2015, 2015.

Gerber, R. P. and Gerber, M. B.: Ingestion of natural particulate organic matter and subsequent assimilation, respiration and growth by tropical lagoon zooplankton, Mar. Biol., 52(1), 33–43, doi:10.1007/BF00386855, 1979.

Gouze, E., Raimbault, P., Garcia, N. and Picon, P.: Nutrient dynamics and primary production in the eutrophic Berre Lagoon (Mediterranean , France), Transitional Waters Bull., 2, 17–40, doi:10.1285/i18252273v2n2p17, 2008.

Gruber, N., Clement, D., Carter, B. R., Feely, R. A., van Heuven, S., Hoppema, M., Ishii, M., Key, R. M., Kozyr, A., Lauvset, S. K., Lo Monaco, C., Mathis, J. T., Murata, A., Olsen, A., Perez, F. F., Sabine, C. L., Tanhua, T. and Wanninkhof, R. H.: The oceanic sink for anthropogenic CO_2 from 1994 to 2007, Science, 363(6432), 1193–1199, doi:10.1126/science.aau5153, 2019.

Gutiérrez-Rodríguez, A., Latasa, M., Scharek, R., Massana, R., Vila, G. and Gasol, J. M.: Growth and grazing rate dynamics of major phytoplankton groups in an oligotrophic coastal site, Estuar. Coast. Shelf Sci., 95(1), 77–87, doi:10.1016/j.ecss.2011.08.008, 2011.

Harrison, W. G., Harris, L. R. and Irwin, B. D.: The kinetics of nitrogen utilization in the oceanic mixed layer: Nitrate and ammonium interactions at nanomolar concentrations, Limnol. Oceanogr., 41(1), 16–32, doi:10.4319/lo.1996.41.1.0016, 1996.

Herrmann, M., Somot, S., Calmanti, S., Dubois, C., and Sevault F.: Representation of spatial and temporal variability of daily wind speed and of intense wind events over the Mediterranean Sea using dynamical downscaling: Impact of the regional climate model configuration, Nat. Hazards Earth Syst. Sci., 11, 1983–2001, doi:10.5194/nhess-11-1983-2011, 2011.

Hoegh-Guldberg, O., Jacob, D., Taylor, M., Bindi, M., Brown, S., Camilloni, I., Diedhiou, A., Djalante, R., Ebi, K., Engelbrecht, F., Guiot, J., Hijioka, Y., Mehrotra, S., Payne, A., Seneviratne, S. I., Thomas, A., Warren, R. and Zhou, G.: Impacts of 1.5°C Global Warming on Natural and Human Systems, in Global warming of 1.5°C. An IPCC Special Report on the impacts of global warming of 1.5°C above pre-industrial levels and related global greenhouse gas emission pathways, in the context of strengthening the global response to the threat of climate change, edited by V. Masson-Delmotte, P. Zhai, H. O. Pörtner, D. Roberts, J. Skea, P. R. Shukla, A. Pirani, W. Moufouma-Okia, C. Péan, R. Pidcock, S. Connors, J. B. R. Matthews, Y. Chen, X. Zhou, M. I. Gomis, E. Lonnoy, T. Maycock, M. Tignor, and

Mis en forme : Centré

T. Waterfield, World Meteorological Organization Technical Document., 2018.

Kapsenberg, L., Alliouane, S., Gazeau, F., Mousseau, L. and Gattuso, J.-P.: Coastal ocean acidification and increasing total alkalinity in the northwestern Mediterranean Sea, Ocean Sci., 13(3), 411–426, doi:10.5194/os-13-411-2017, 2017.

Lacroix, G. and Grégoire, M.: Revisited ecosystem model (MODECOGeL) of the Ligurian Sea: seasonal and interannual variability due to atmospheric forcing, J. Mar. Syst., 37(4), 229–258, doi:10.1016/S0924-7963(02)00190-2, 2002.

Leblanc, K., Quéguiner, B., Diaz, F., Cornet, V., Michel-Rodriguez, M., Durrieu de Madron, X., Bowler, C., Malviya, S., Thyssen, M., Grégori, G., Rembauville, M., Grosso, O., Poulain, J., de Vargas, C., Pujo-Pay, M. and Conan, P.: Nanoplanktonic diatoms are globally overlooked but play a role in spring blooms and carbon export, Nat. Commun., 9(1), 953, doi:10.1038/s41467-018-03376-9, 2018.

Lueker, T. J., Dickson, A. G. and Keeling, C. D.: Ocean pCO_2 calculated from dissolved inorganic carbon, alkalinity, and equations for K1 and K2: Validation based on laboratory measurements of CO_2 in gas and seawater at equilibrium, Mar. Chem., 70(June 2015), 105–119, doi:10.1016/S0304-4203(00)00022-0, 2000.

Margalef, R.: Life-forms of phytoplankton as survival alternatives in an unstable environment, edited by Gauthier-Villars, Oceanol. Acta, 1(4), 493–509 [online] Available from: https://archimer.ifremer.fr/doc/00123/23403/, 1978.

Marty, J.-C., Chiavérini, J., Pizay, M.-D. and Avril, B.: Seasonal and interannual dynamics of nutrients and phytoplankton pigments in the western Mediterranean Sea at the DYFAMED time-series station (1991–1999), Deep Sea Res. Part II Top. Stud. Oceanogr., 49(11), 1965–1985, doi:10.1016/S0967-0645(02)00022-X, 2002.

Matthews, H. D., Gillett, N. P., Stott, P. a and Zickfeld, K.: The proportionality of global warming to cumulative carbon emissions., Nature, 459(7248), 829–32, doi:10.1038/nature08047, 2009.

Mella-Flores, D., Mazard, S., Humily, F., Partensky, F., Mahé, F., Bariat, L., Courties, C., Marie, D., Ras, J., Mauriac, R., Jeanthon, C., Mahdi Bendif, E., Ostrowski, M., Scanlan, D. J. and Garczarek, L.: Is the distribution of Prochlorococcus and Synechococcus ecotypes in the Mediterranean Sea affected by global warming?, Biogeosciences, 8(9), 2785–2804, doi:10.5194/bg-8-2785-2011, 2011.

Middelburg, J. J.: Marine ~~Carbon Biogeochemistry A Primer~~carbon biogeochemistry a primer for ~~Earth System Scientists~~earth system scientists, Springer B., edited by Springer Briefs in Earth System Sciences, Springer Briefs in Earth System Sciences, 2019.

Millero, F. J.: Thermodynamics Seawater - 1. The PVT Properties, *Ocean Science and Engineering*, *7*(4), 403-460 1982.

Millero, F. J.: Thermodynamics of the carbon dioxide system in the oceans, Geochim. Cosmochim. Acta, 59(4), 661–677, doi:10.1016/0016-7037(94)00354-O, 1995.

Millet, B., Pinazo, C., Daniela, B., Remi, P., Pierre, G. and Ivane, P.: Unexpected spatial impact of treatment plant discharges induced by episodic hydrodynamic events: Modelling Lagrangian transport of fine particles by Northern Current intrusions in the bays of Marseille (France), edited by P. L. Science, PLoS One, 13(4), e0195257 (25p.), doi:10.1371/journal.pone.0195257, 2018.

Millot, C.: The Gulf of Lions hydrodynamics, Cont. Shelf Res., 10(9), 885–894, doi:10.1016/0278-4343(90)90065-T, 1990.

Monterey, G. and Levitus, S.: Seasonal ~~Variability~~variability of ~~Mixed Layer Depth~~mixed layer depth for the World Ocean, NOAA Atlas NESDIS 14, Washington, D. C., 1997.

Moran, M. A.: The global ocean microbiome, Sci. Am. Assoc. Adv. Sci., 350(6266), doi:10.1126/science.aac8455, 2015.

Morris, A. W. and Riley, J. P.: The bromide/chlorinity and sulphate/chlorinity ratio in sea water, Deep Sea Res. Oceanogr. Abstr., 13(4), 699–705, doi:10.1016/0011-7471(66)90601-2, 1966.

Mucci, A.: The solubility of calcite and aragonite in seawater at various salinities, temperatures, and one atmosphere total pressure, Am. J. Sci., 283(7), 780–799, doi:10.2475/ajs.283.7.780, 1983.

Orr, J. C., Fabry, V. J., Aumont, O., Bopp, L., Doney, S. C., Feely, R. A., Gnanadesikan, A., Gruber, N., Ishida, A., Joos, F., Key, R. M., Lindsay, K., Maier-Reimer, E., Matear, R., Monfray, P., Mouchet, A., Najjar, R. G., Plattner, G.-K., Rodgers, K. B., Sabine, C. L., Sarmiento, J. L., Schlitzer, R., Slater, R. D., Totterdell, I. J., Weirig, M.-F., Yamanaka, Y. and Yool, A.: Anthropogenic ocean acidification over the twenty-first century and its impact on calcifying organisms, Nature, 437(7059), 681–6, doi:10.1038/nature04095, 2005.

Pairaud, I., Gatti, J., Bensoussan, N., Verney, R. and Garreau, P.: Hydrology and circulation in a coastal area off Marseille: Validation of a nested 3D model with observations, J. Mar. Syst., 88(1), 20–33, doi:10.1016/j.jmarsys.2011.02.010, 2011.

Para, J., Coble, P. G., Charrière, B., Tedetti, M., Fontana, C. and Sempéré, R.: Fluorescence and absorption properties of chromophoric dissolved organic matter (CDOM) in coastal surface waters of the northwestern Mediterranean Sea, influence of the Rhône River, Biogeosciences, 7(12), 4083–4103, doi:10.5194/bg-7-4083-2010, 2010.

Petrenko, A.: Variability of circulation features in the Gulf of Lion, NW Mediterranean Sea . Importance of inertial currents ~~Variabilité de la circulation dans le golfe du Lion (Méditerranée nord-occidentale). Importance des courants d ' inertie.~~, Oceanol. Acta, 26, 323–338, doi:10.1016/S0399-1784(03)00038-0, 2003.

Mis en forme : Centré

Pont, D., Simonnet, J.-P. and Walter, A. V~~.~~: Medium-term ~~Changes~~changes in ~~Suspended Sediment Delivery~~suspended sediment delivery to the Ocean: Consequences of ~~Catchment Heterogeneity~~catchment heterogeneity and ~~River Management~~river management (Rhône River, France), Estuar. Coast. Shelf Sci., 54(1), 1–18, doi:10.1006/ecss.2001.0829, 2002.

Le Quéré, C., Andrew, R. M., Friedlingstein, P., Sitch, S., Hauck, J., Pongratz, J., Pickers, P. A., Korsbakken, J. I., Peters, G. P., Canadell, J. G., Arneth, A., Arora, V. K., Barbero, L., Bastos, A., Bopp, L., Chevallier, F., Chini, L. P., Ciais, P., Doney, S. C., Gkritzalis, T., Goll, D. S., Harris, I., Haverd, V., Hoffman, F. M., Hoppema, M., Houghton, R. A., Hurtt, G., Ilyina, T., Jain, A. K., Johannessen, T., Jones, C. D., Kato, E., Keeling, R. F., Goldewijk, K. K., Landschützer, P., Lefèvre, N., Lienert, S., Liu, Z., Lombardozzi, D., Metzl, N., Munro, D. R., Nabel, J. E. M. S., Nakaoka, S.-I., Neill, C., Olsen, A., Ono, T., Patra, P., Peregon, A., Peters, W., Peylin, P., Pfeil, B., Pierrot, D., Poulter, B., Rehder, G., Resplandy, L., Robertson, E., Rocher, M., Rödenbeck, C., Schuster, U., Schwinger, J., Séférian, R., Skjelvan, I., Steinhoff, T., Sutton, A., Tans, P. P., Tian, H., Tilbrook, B., Tubiello, F. N., van der Laan-Luijkx, I. T., van der Werf, G. R., Viovy, N., Walker, A. P., Wiltshire, A. J., Wright, R., Zaehle, S. and Zheng, B.: Global Carbon Budget 2018, Earth Syst. Sci. Data, 10(4), 2141–2194, doi:10.5194/essd-10-2141-2018, 2018.

Raven, J. A. and Falkowski, P. G.: Oceanic sinks for atmospheric CO_2, Plant. Cell Environ., 22(6), 741–755, doi:10.1046/j.1365-3040.1999.00419.x, 1999.

Riley, J. P.: The occurrence of anomalously high fluoride concentrations in the North Atlantic, Deep Sea Res. Oceanogr. Abstr., 12(2), 219–220, doi:10.1016/0011-7471(65)90027-6, 1965.

Riley, J. P. and Tongudai, M.: The major cation/chlorinity ratios in sea water, Chem. Geol., 2, 263–269, doi:10.1016/0009-2541(67)90026-5, 1967.

Roobaert, A., Laruelle, G. G., Landschützer, P., Gruber, N., Chou, L. and Regnier, P.: The ~~Spatiotemporal Dynamics~~spatiotemporal dynamics of the ~~Sources~~sources and ~~Sinks~~sinks of CO_2 in the ~~Global Coastal Ocean~~global coastal ocean, Global Biogeochem. Cycles, 33, doi:10.1029/2019GB006239, 2019.

Ross, O. N., Fraysse, M., Pinazo, C. and Pairaud, I.: Impact of an intrusion by the Northern Current on the biogeochemistry in the eastern Gulf of Lion, NW Mediterranean, Estuar. Coast. Shelf Sci., 170, 1–9, doi:10.1016/j.ecss.2015.12.022, 2016.

Rykiel, E. J.: Testing ecological models: The meaning of validation, Ecol. Modell., 90(3), 229–244, doi:10.1016/0304-3800(95)00152-2, 1996.

Sarthou, G., Timmermans, K. R., Blain, S. and Tréguer, P.: Growth physiology and fate of diatoms in the ocean: a review, J. Sea Res., 53(1), 25–42, doi:10.1016/j.seares.2004.01.007, 2005.

Schneider, A., Wallace, D. W. R. and Körtzinger, A.: Alkalinity of the Mediterranean Sea, Geophys. Res. Lett., 34(15), doi:10.1029/2006GL028842, 2007.

Sempéré, R., Charrière, B., van Wambeke, F., and Cauwet, G.: Carbon inputs of the Rhône River to the Mediterranean Sea: Biogeochemical implications, Global Biogeochem. Cycles, 14(2), 669-681, doi:10.1029/1999GB900069, 2000.

Small, C. and Nicholls, R. J.: A ~~Global Analysis of Human Settlement~~global analysis of human settlement in ~~Coastal Zones~~coastal zones, J. Coast. Res., 19(3), 584–599 [online] Available from: http://www.jstor.org/stable/4299200, 2003.

Smith, C. L. and Tett, P.: A depth-resolving numerical model of physically forced microbiology at the European shelf edge, J. Mar. Syst., 26(1), 1–36, doi:10.1016/S0924-7963(00)00010-5, 2000.

Soetaert, K., Hofmann, A. F., Middelburg, J. J., Meysman, F. J. R. and Greenwood, J.: The effect of biogeochemical processes on pH, Mar. Chem., 105(1–2), 30–51, doi:10.1016/j.marchem.2006.12.012, 2007.

Tett, P.: A three-layer vertical and microbiological processes model for shelf seas., 1990.

Tett, P., Droop, M. R. and Heaney, S. I.: The Redfield ~~Ratio~~ratio and ~~Phytoplankton Growth Rate~~phytoplankton growth rate, J. Mar. Biol. Assoc. United Kingdom, 65(2), 487–504, doi:10.1017/S0025315400050566, 1985.

Thingstad, T. F.: Utilization of N, P, and organic C by heterotrophic bacteria . I. Outline of a chemostat theory with a consistent concept of "maintenance" metabolism, Mar. Ecol. Prog. Ser., 35, 99–109, doi:10.3354/meps035099, 1987.

Uppström, L. R.: The boron/chlorinity ratio of deep-sea water from the Pacific Ocean, Deep Sea Res. Oceanogr. Abstr., 21(2), 161–162, doi:10.1016/0011-7471(74)90074-6, 1974.

Upstill-Goddard, R. C.: Air-sea gas exchange in the coastal zone, Estuar. Coast. Shelf Sci., 70(3), 388–404, doi:10.1016/j.ecss.2006.05.043, 2006.

Wanninkhof, R. H.: Relationship ~~Between Wind Speed~~between wind speed and ~~Gas Exchange~~gas exchange, J. Geophys. Res., 97(C5), 7373–7382, 1992.

Weiss, R. F.: Carbon dioxide in water and seawater: the solubility of a non-ideal gas, Mar. Chem., 2(3), 203–215, doi:10.1016/0304-4203(74)90015-2, 1974.

Willmott, C. J.: Some comments on the evaluation of model performance, Bull. Am. Meteorol. Soc., 63(11), 1982.

Wimart-Rousseau, C., Lajaunie-Salla, K., Marrec, P., Wagener, T., Raimbault, P., Lagadec, V., Lafont, M., Garcia, N., Diaz, F., Pinazo, C., Yohia, C., Garcia, F., Xueref-Remy, I., Blanc, P. E., Armengaud, A. and Lefèvre, D.: Temporal variability of the carbonate system and air-sea CO_2 exchanges in a Mediterranean human-impacted coastal site, Estuar. Coast. Shelf Sci., 236(February), doi:10.1016/j.ecss.2020.106641, 2020.

Mis en forme : Indice

Mis en forme : Centré

Xueref-Remy, I., Milne, M., Zoghbi, N., Yohia, C., Armengaud, A., Blanc, P.-E., Delmotte, M., Piazzola, J., Nathan, B., Ramonet, M. and Lac, C.: Assessing atmospheric CO_2 variability in the Aix-Marseille metropolis area (France) and its coastal Mediterranean Sea at different time scales within the AMC project, Prague, Aus, [online] Available from: https://conference.icos-ri.eu/wp-ontent/uploads/2018/09/ICOS2018SC_Book_of_Abstracts.pdf, 2018a.

Xueref-Remy, I., Dieudonné, E., Vuillemin, C., Lopez, M., Lac, C., Schmidt, M., Delmotte, M., Chevallier, F., Ravetta, F., Perrussel, O., Ciais, P., Bréon, F., Broquet, G., Ramonet, M. and Ampe, C.: Diurnal , synoptic and seasonal variability of atmospheric CO_2 in the Paris megacity area, Atmos. Chem. Phys., 18, 3335–3362, doi:10.5194/acp-18-3335-2018, 2018b.

Yohia, C.: Genèse du mistral par interaction barocline et advection du tourbillon potentiel, Climatologie, 13, 24–37 [online] Available from: https://doi.org/10.4267/climatologie.1182, 2017.

Zappa, C. J., Raymond, P. A., Terray, E. A. and McGillis, W. R.: Variation in ~~Surface Turbulence~~surface turbulence and the ~~Gas Transfer Velocity~~gas transfer velocity over a ~~Tidal Cycle~~tidal cycle in a ~~Macro~~macro-tidal ~~Estuary~~estuary, Estuaries, 26(6), 1401–1415, 2003.

Mis en forme : Centré

Tables

	Temperature	Wind	River input	Atmospheric CO_2
S0 – Reference	In situ data of 2017	WRF model 2017	No	CAV station 2017
S1 - T increases	In situ data of 2017 +1.5°C	WRF model 2017	No	CAV station 2017
S2 - Wind constant	In situ data of 2017	7 m s^{-1}	No	CAV station 2017
S3 - Wind events	In situ data of 2017	3 days ~~of~~at 20 m s^{-1}	No	CAV station 2017
S4 - NO_3	In situ data of 2017	WRF model 2017	Yes, NO_3 ~~inputs~~	CAV station 2017
~~**S5 – TA**~~	~~In situ data of 2017~~	~~WRF model 2017~~	~~TA inputs~~	~~CAV station 2017~~
~~**S6**~~**S5 - Non-urban**	In situ data of 2017	WRF model 2017	No	OHP station 2017

Table 1: Forcing of the different scenarios (S) simulated with the model. See section 2.4 for details of scenarios.

	Chl	seawater pCO_2	pH	DIC	TA
Obs min-max	[0.10– 1.71]	[358 – 471]	[8.014 – 8.114]	[2260 – 2348]	[2561 – 2624]
Mod min-max	[0.03 – 0.73]	[331 – 522]	[7.979 – 8.171]	[2220 – 2323]	[2560– 2572]
Bias	-0.22	22.47	-0.016	-8.48	-24.91
WSS	0.36	0.69*	0.75*	0.71*	0.43
N	22	20	21	20	20

Table 2: Statistical evaluation of observations *vs.* model for 2017 year: observed and simulated minimum and maximum values, WSS = Wilmott Skill Score, N = number of measurements. Units of bias are those of modeled variables: chlorophyll *a* (Chl, mg m^{-3}), seawater pressure of CO_2 (seawater pCO_2, µatm), *p*H, dissolved inorganic carbon (DIC, µmol kg^{-1}) and total alkalinity (TA, µmol kg^{-1}~~) .~~). *significant value of WSS (> 0.70).

		Aeration	GPP	R_A	R_H	R	NEP
Mean flux	**Year**	0.017	-0.413	0.065	0.348	0.413	0
	MWC	-0.245	-0.314	0.052	0.176	0.228	0.086
	SWC	0.405	-0.521	0.079	0.555	0.634	-0.113
Contribution	**Year**	78%	11%	2%	9%	11%	~~/~~

Table 3: Mean flux values (mmol m^{-3} d^{-1}) and the contribution of each process to the DIC variations for the reference simulation over the year and SWC/MWC periods. GPP: Gross primary production, R_A: Autotroph respiration, R_H: heterotroph respiration, NEP: Net Ecosystem Production

Mis en forme : Police :Italique

Mis en forme : Centré

Figures

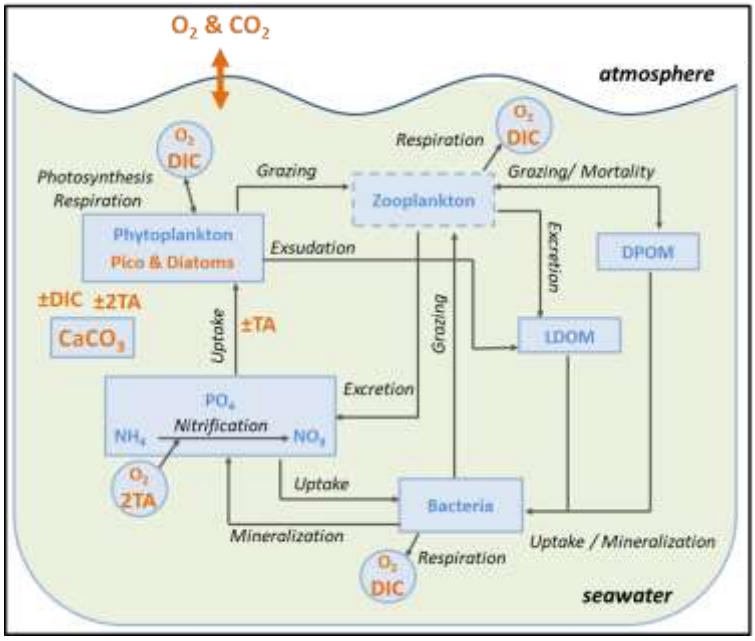

Figure 1: Schematic diagram of the biogeochemical model Eco3M-CarbOx. Explicit state variables of the model are indicated in continuous-line box or circles except the implicit variable for zooplankton (dotted line box). Orange-written state variables are added variables compared to the preexisting biogeochemical model of Fraysse et al. (2013). Arrows represent processes between two state variables. TA: Total Alkalinity. DIC: Dissolved Inorganic Carbon, CO_2: carbon dioxide, O_2: Oxygen, $CaCO_3$: calcium carbonate.

Mis en forme : Centré

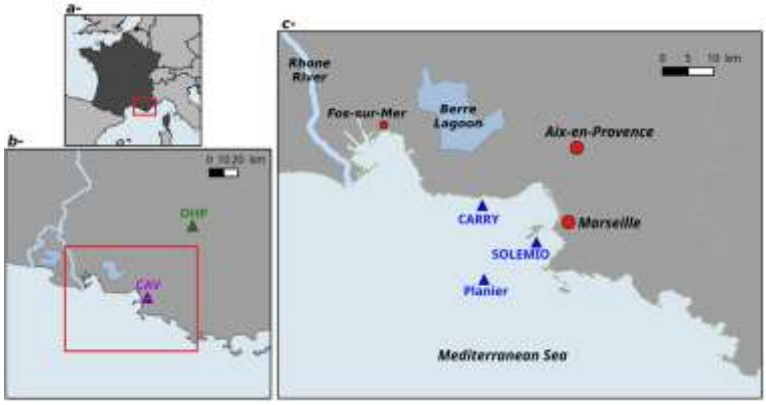

Figure 2: Map of study area: The Region Sud (A), Aix-Marseille Metropolis (B), the Bay of Marseille (C). CAV= Cinq AVenues Station (urban site), OHP: Observatoire de Haute Provence station (non-urban site), Carry, Solemio, Planier: ~~Study~~Marine study sites ~~at sea~~ in the Bay of Marseille.

Mis en forme : Centré

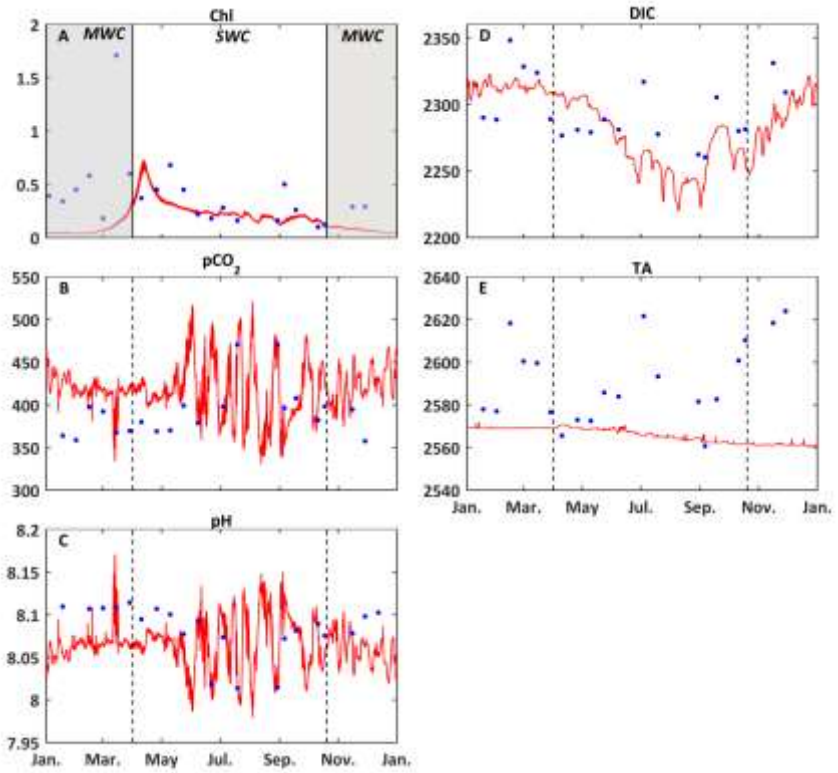

Figure 3: Comparison of model results (red) and *in situ* data (blue) at the surface of the SOLEMIO station. (A) Chlorophyll-*a* concentrations (mg m^{-3}), (B) pCO_2 (µatm), (C) *p*H, (D) DIC (µmol kg^{-1}), (E) TA (µmol kg^{-1}). The value of each state variable represents the mean around ±5 days of the sampling date~~, and the error bars are the standard deviation of values over this time period.~~. The shaded area and dotted black line delimit the SWC and MWC periods.

Mis en forme : Police :Italique

Mis en forme : Centré

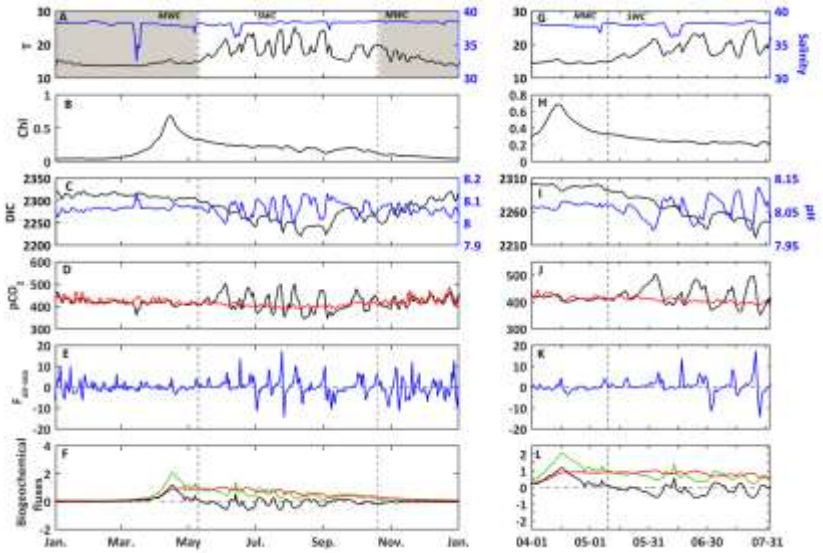

Figure 4: In the left panels: year 2017, right panels: temporal focus between April 1st and July 31th, 2017. *In situ* daily average of (A, G) temperature (°C, black line) and salinity (blue line) at the SOLEMIO station~~.~~ (at the surface). Modeled daily average (B, H) chlorophyll *a* concentrations (mg m^{-3}, black line) (C, I) DIC (µmol kg^{-1}, black line) and *p*H (blue line), (D, J) seawater pCO_2 (µatm, black line) and atmosphere pCO_2 from OHP (µatm, red line), (E, K) air-sea CO_2 fluxes mmol m^{-3} d^{-1}), (F, L) Gross Primary Production (mmol m^{-3} d^{-1}, green line), total respiration (mmol m^{-3} d^{-1}, red line) and Net Ecosystem Production (mmol m^{-3} d^{-1}, black line). The shaded areas and dotted black lines delimit the SWC and MWC periods.

Mis en forme : Centré

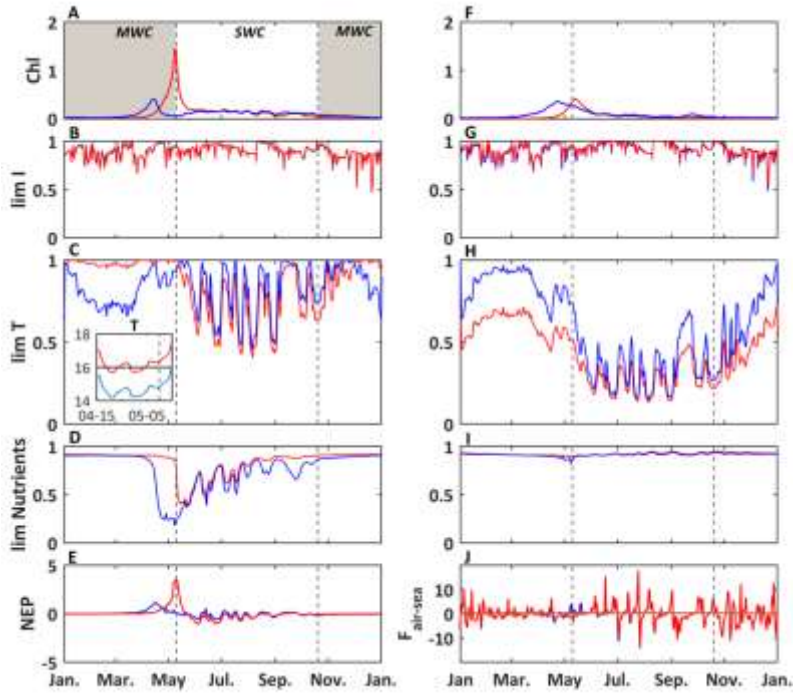

Figure 5: Modeled daily average chlorophyll *a* concentrations (mg m^{-3}) (A), light limitation (B), temperature limitation, and a zoom from April 15th to May 5th of temperature (C) and nutrient limitation (D) for picophytoplankton and the same set for diatoms (F, G, H and I). Modeled daily average NEP (mmol m^{-3} d^{-1}, E) and air-sea CO_2 flux (mmol m^{-3} d^{-1}, J). Reference simulation (S0, blue line) and temperature-shifted simulation by 1.5°C (S2, red line). The shaded area and dotted black lines delimit the SWC and MWC periods.

Mis en forme

Mis en forme : Centré

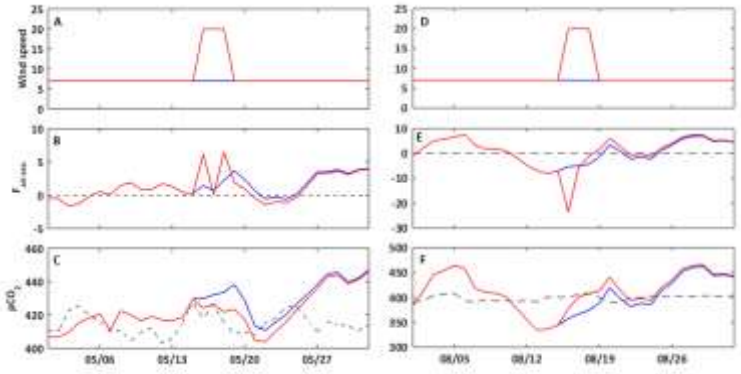

Figure 6: Temporal evolution for May (left panels) and August (right panels) 2017 of the wind speed (m s^{-1}, A, D); air-sea CO_2 fluxes (mmol m^{-3} d^{-1}, B, E); seawater partial pressure of CO_2 (µatm, C, F). Constant wind scenario (S2, blue line) and wind event scenario (S3, red line). On panels C and F, the dashed line represents the atmosphere partial pressure of CO_2 (µatm) at the CAV station.

Mis en forme : Centré

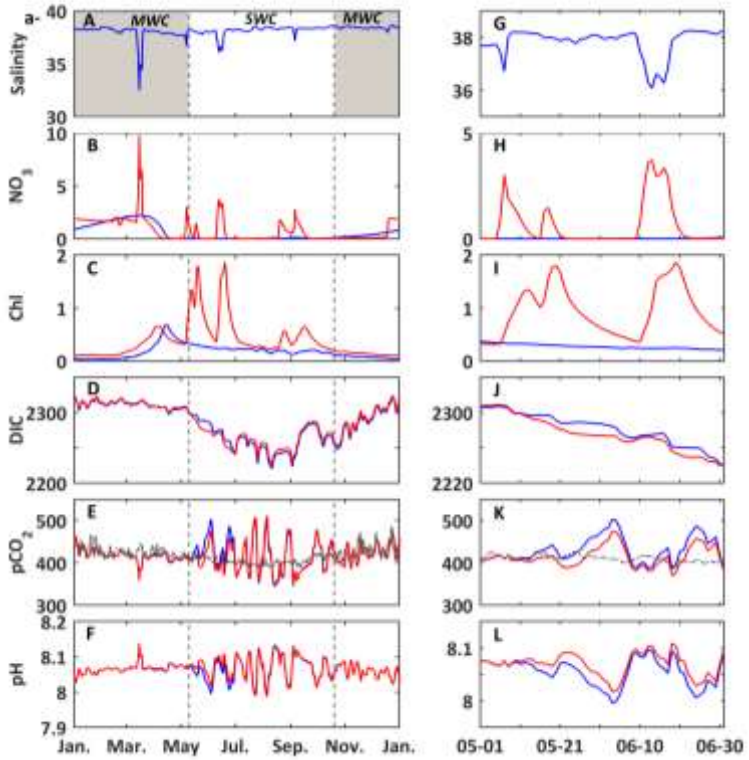

Figure 7: In the left panels: year 2017 and right panels: temporal focus between May 1st and July 1st, 2017. (A, G) *In situ* daily average of salinity. Modeled daily average (B, H) nitrate concentrations (mmol m^{-3}); (C, I) chlorophyll *a* concentrations (mg m^{-3}); (D, J) DIC (µmol kg^{-1}); (E, K) seawater pCO_2 (µatm), and (F, L) *p*H. Reference simulation (S0, blue line) and nitrate supply simulation (S4, red line). On panels E and K, the dashed line represents the atmosphere partial pressure of CO_2 (µatm) at the CAV station. The shaded area and dotted black lines delimit the SWC and MWC periods.

Mis en forme : Centré

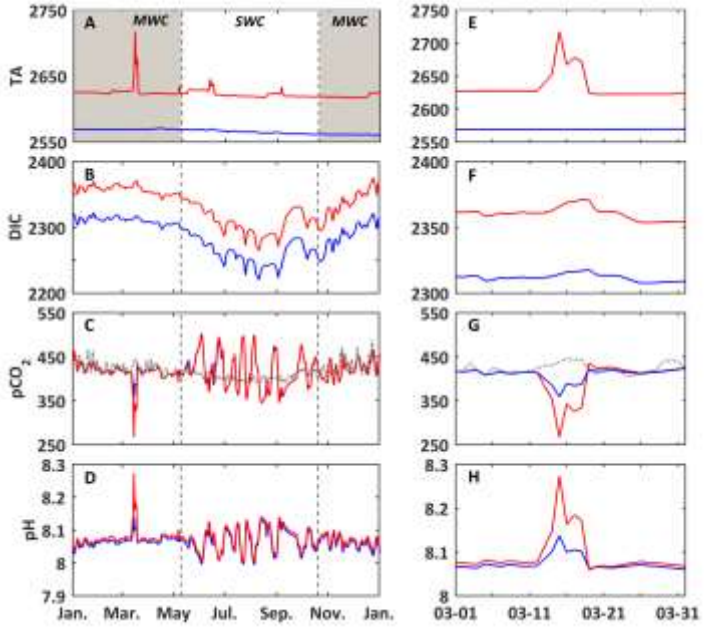

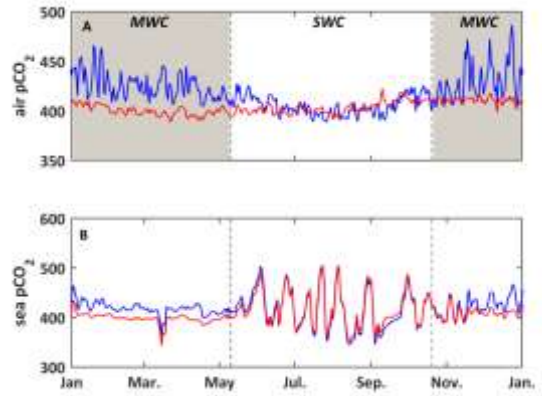

Figure 8: ~~In the left for the whole year 2017 and in the right between March 1st and April 1st, 2017. Modelled daily average (A, E) TA (µmol kg^{-1}); (B, F) DIC (µmol kg^{-1}); (C, G) seawater pCO_2 (µatm), and (D, H) pH. Reference simulation (S0, blue line) and alkalinity supply simulation (S5, red line). On the panels C and G, the dashed line represents the atmosphere partial pressure of CO_2 (µatm) at the CAV station. The shaded area and dotted black lines delimit the SWC and MWC periods.~~

Mis en forme : Centré

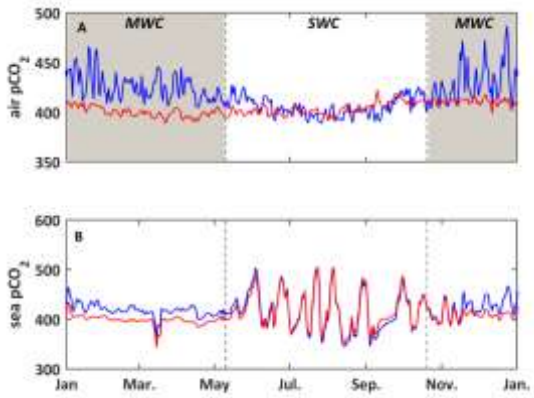

~~Figure 9:~~ (A) Temporal evolution for the year 2017 of the observed partial pressure of CO_2 (µatm) in the atmosphere ~~in µatm~~ at the CAV station, called the "urban scenario" (S0, blue line), and at the OHP station, called the "non-urban scenario", and in seawater (S6, red line). (B) Temporal evolution for the year 2017 of the modeled seawater partial pressure of CO_2 (µatm) with forcings from the urban (S0, blue line) and non-urban (S6, red line) scenarios. The shaded area and dotted black lines delimit the SWC and MWC periods.

Mis en forme : Centré

Appendix A: Details of resolution of carbonate system module

A.1. Calculation of carbonate systems constants:

Mis en forme : Retrait : Gauche : 0,5 cm, Sans numérotation ni puces

- ~~Concentration in~~ Total Fluoride (TF) ~~ions~~concentrations from Riley (1965**)** in mol kg^{-1}:

$$TF = \frac{0.000067}{18.998} \cdot \frac{S}{1.80655}$$

- ~~Concentration in~~ Total Sulphate (TS) ~~ions~~concentration from Morris and Riley (1966) in mol kg^{-1}:

$$TS = \frac{0.14}{96.062} \cdot \frac{S}{1.80655}$$

- Calcium ion concentration from Riley and Tongudai (1967) in mol kg^{-1}:

$$Ca^{2+} = \frac{0.02128}{40.087} \cdot \frac{S}{1.80655}$$

- ~~Concentration in~~ Total Boron (TB) ~~ions~~concentration from Uppström (1974) in mol kg^{-1}:

$$TB = \frac{0.000416 \cdot \mathrm{S}}{35}$$

- Ionic Strength (IonS) from Millero (1982):

$$IonS = \frac{19.924 \cdot \mathrm{S}}{1000 - 1.005 \cdot \mathrm{S}}$$

The constants are calculated ~~in~~on the total *p*H scale except for K_S ~~in~~on free *p*H scale

- If necessary, pH scale conversion factors are following:

From Seawater *p*H Scale (SWS) to total *p*H scale: $\mathrm{SWStoTOT} = \frac{1+\frac{TS}{K_S}}{1+\frac{TS}{K_S}+\frac{TF}{K_F}}$

From Free *p*H Scale to Total *p*H scale: $FREEtoTOT = 1 + \frac{TS}{K_S}$

- K_S equilibrium constant of dissociation of HSO_4^- from Dickson (1990a) in mol kg^{-1}:

$$K_S = \frac{-4276.1}{T_{(K)}} + 141.328 - 23.093 \cdot \log(T_{(K)}) + \left(324.57 - 47.986 \cdot \log(T_{(K)}) - \frac{13856}{T_{(K)}}\right) \cdot Ions^2$$

$$K_S = K_S + \left(-771.54 + 114.723 \cdot \log(T_{(K)}) + \frac{35474}{T_{(K)}}\right) \cdot Ions + \frac{-2698}{T_{(K)}} \cdot ~~Ions^{1.5}~~ + ~~\frac{1776}{T_{(K)}}~~ Ions^{\frac{3}{2}} + \frac{1776}{T_{(K)}} \cdot Ions^2$$

$$K_S = e^{K_S} \cdot (1 - 0.001005 \cdot S)$$

- K_F equilibrium constant of dissociation of hydrogen fluoride ~~ions~~ (HF) formation from Dickson and Riley (1979) in mol kg^{-1}:

~~$K_F = e^{\frac{1590.2}{T_{(K)}} - 12.641 + 1.525 \cdot Ions^{1.5}} \cdot (1 - 0.001005 \cdot S)$~~ $K_F = e^{\frac{1590.2}{T_{(K)}} - 12.641 + 1.525 \cdot Ions^{\frac{1}{2}}} \cdot (1 - 0.001005 \cdot S)$

- K_B equilibrium constant of dissociation of boric acid from Dickson (1990b) in mol kg^{-1}

$$K_B = (-8966.9 - 2890.53 \cdot S^{\frac{1}{2}} - 77.942 \cdot S + 1.728 \cdot S^{\frac{3}{2}} - 0.0996 \cdot S^2)/T_{(K)}$$

$$K_B = K_B + 148.0248 + 137.1942 \cdot S^{\frac{1}{2}} + 1.62142 \cdot S + (-24.4344 - 25.085 \cdot S^{\frac{1}{2}} - 0.2474 \cdot S) \cdot \log(T) + 0.053105 \cdot S^{\frac{1}{2}} \cdot T$$

- K_0 constant of CO_2 solubility from Weiss (1974) in mol kg^{-1} atm^{-1}:

$$K_0 = \exp\left(-60.2409 + 93.4517 \cdot \frac{100}{T_{(K)}} + 23.3585 \cdot \log\left(\frac{T_{(K)}}{100}\right) + S \cdot \left(0.023517 - 0.023656 \cdot \frac{T_{(K)}}{100} + 0.0047036 \cdot \left(\frac{T_{(K)}}{100}\right)^2\right)\right)$$

- K_e: Dissociation constant of water from Millero (1995) in (mol kg^{-1})^2 :

$$K_e = \exp\left(\frac{-13847.26}{T_{(K)}} + 148.9802 - 23.6521 \cdot \log\left(T_{(K)}\right) + \left(-5.977 + \frac{118.67}{T_{(K)}} + 1.0495 \cdot \log\left(T_{(K)}\right)\right) \cdot S^{1/2} - 0.01615 \cdot S\right)$$

$K_e = K_e \cdot SWStoTOT$, in total pH scale in mol kg^{-1}

- K_1 and K_2 from Lueker et al. (2000) in mol kg^{-1}:

$$K_1 = 10^{\frac{-3633.86}{T_{(K)}} + 61.2172 - 9.6777 \cdot \log\left(T_{(K)}\right) + 0.011555 \cdot S - 0.0001152 \cdot S^2}$$

$$K_2 = 10^{\frac{-471.78}{T_{(K)}} + 251.929 - 3.16967 \cdot \log\left(T_{(K)}\right) + 0.01781 \cdot S - 0.0001122 \cdot S^2}$$

- K_{ca} for calcite from Mucci (1983) in (mol kg^{-1})^2:

K_{ca}

$$= 10^{-171.9065 - 0.077993 \cdot T_{(K)} + \frac{2839.319}{T_{(K)}} + 71.595 \cdot log10\left(T_{(K)}\right) + (-0.77712 + 0.0028426 \cdot T_{(K)} + \frac{178.34}{T_{(K)}}) \cdot S^{\frac{1}{2}} - 0.07711 \cdot S + 0.0041249 \cdot S^{1.5}} \quad 10^{-171.9065 - 0.077993 \cdot T_{(K)} + \frac{2839.319}{T_{(K)}} + 71.595 \cdot log10\left(T_{(K)}\right) + (-0.77712 + 0.002842}$$

- All the constants are corrected by the effect of hydrostatic pressure:

$R = 83.1451$ in ml bar^{-1} K^{-1} mol^{-1}

$$lnK_1fac = \frac{\left(25.5 - 0.1271 \cdot T_{(°C)} + 0.5 \cdot \left(\frac{-3.08 + 0.0877 \cdot T_{(°C)}}{1000}\right) \cdot P_{bar}\right) \cdot P_{bar}}{R * T_{(K)}};\ K_1 = K_1 \cdot e^{lnK_1fac}$$

$$lnK_2fac = \frac{\left(15.82 - 0.0219 \cdot T_{(°C)} + 0.5 \cdot \left(\frac{1.13 + 0.1475 \cdot T_{(°C)}}{1000}\right) \cdot P_{bar}\right) \cdot P_{bar}}{R \cdot T_{(K)}};\ K_2 = K_2 \cdot e^{lnK_2fac}$$

$$lnK_Bfac = \frac{\left(29.48 - 0.1622 \cdot T_{(°C)} + 0.002608 \cdot T_{(°C)}^2 + 0.5 \cdot \left(\frac{-2.84}{1000}\right) \cdot P_{bar}\right) \cdot P_{bar}}{R \cdot T_{(K)}};\ K_B = K_B \cdot e^{lnK_Bfac}$$

$$lnK_efac = \frac{\left(20.02 - 0.1119 \cdot T_{(°C)} + 0.001409 \cdot T_{(°C)}^2 + 0.5 \cdot \left(\frac{-5.13 + 0.0794 \cdot T_{(°C)}}{1000}\right) \cdot P_{bar}\right) \cdot P_{bar}}{R \cdot T_{(K)}};\ K_e = K_e \cdot e^{lnK_efac}$$

$$lnK_Ffac = \frac{\left(9.78 - 0.009 \cdot T_{(°C)} + 0.0009429 \cdot T_{(°C)}^2 + 0.5 \cdot \left(\frac{-3.91 + 0.054 \cdot T_{(°C)}}{1000}\right) \cdot P_{bar}\right) \cdot P_{bar}}{R \cdot T_{(K)}};\ K_F = K_F \cdot e^{lnK_Ffac}$$

$$lnK_Sfac = \frac{\left(18.03 - 0.0466 \cdot T_{(°C)} + 0.000316 \cdot T_{(°C)}^2 + 0.5 \cdot \left(\frac{-4.53 + 0.009 \cdot T_{(°C)}}{1000}\right) \cdot P_{bar}\right) \cdot P_{bar}}{R \cdot T_{(K)}};\ K_S = K_S \cdot e^{lnK_Sfac}$$

$$lnK_cafac = \frac{\left(48.76 - 0.5304 \cdot T_{(°C)} + 0.5 \cdot \left(\frac{-11.76 + 0.3692 \cdot T_{(°C)}}{1000}\right) \cdot P_{bar}\right) \cdot P_{bar}}{R \cdot T_{(K)}};\ K_{ca} = K_{ca} \cdot e^{lnK_cafac}$$

- Calculation of the Fugacity factor:

We suppose that the pressure is at one atmosphere or close to it (Weiss, 1974):

$P_{atm} = 1.01325\ bar$

$delta = 57.7 - 0.118 \cdot T$ in cm^3 mol^{-1}

$b = -1636.75 + 12.0408 \cdot \mathrm{T} - 0.0327957 \cdot T^2 + 3.16528 \cdot 0.00001 \cdot T^3$ in cm^3 mol^{-1}

$$FugFac = exp^{\frac{(b + 2 \cdot delta) \cdot P_{atm}}{R \cdot T}}$$

A.2. Resolution of carbonate system

Mise en forme : Police :10,5 pt
Mise en forme : Police :10,5 pt
Mise en forme : Police :10,5 pt
Mise en forme : Police :10,5 pt
Mise en forme : Police :10,5 pt
Mise en forme : Police :10,5 pt
Mise en forme : Police :10,5 pt
Mise en forme : Police :10,5 pt
Mise en forme : Police :10,5 pt
Mise en forme : Sans numérotation ni puces

To resolve the carbonate system, we calculate the $deltapH$, which is the difference of pH between two iterations of the model. We initialize the run by imposing a pH value of 8.

$if\ (nbiter < 1)\ pH = 8$

$pHtol = 0.001$! tolerance for iterations end

$deltapH = pHtol + 1$

$do\ while\ (abs(deltapH) > 0.0001)$

$H = 10^{-pH}$

$Denom = H^2 + K_1 \cdot H + K_1 \cdot K_2$

$CAlk = DIC \cdot K_1 \cdot (\frac{H + 2 \cdot K_2}{Denom})$

$BAlk = \frac{TB \cdot K_B}{K_B + H}$

$OH = \frac{K_e}{H}$

$FreetoTot = 1 + \frac{TS}{K_S}$

$Hfree = \frac{H}{FreetoTot}$

$HSO_4 = \frac{TS}{1 + \frac{K_S}{Hfree}}$

$HF = \frac{TF}{1 + \frac{K_F}{Hfree}}$

$Residual = TA - CAlk - BAlk - OH + Hfree + HSO_4 + HF$

$Slope = DIC \cdot H \cdot K_1 \cdot (H^2 + K_1 \cdot K_2 + 4 \cdot H \cdot K_2)$

$Slope = \frac{Slope}{Denom^2} + OH + H + \frac{BAlk \cdot H}{K_B + H}$

$Slope = \log 10 \cdot \text{Slope}$

$deltapH = Residual/Slope$! this is Newton's method

$do\ while\ (abs(deltapH) > 1)\ deltapH = \frac{deltapH}{2}$! to keep the jump from being too big

$enddo$

$pH = pH + deltapH$! Is on the same scale as K_1 and K_2 were calculated, *i.e.* total *p*H scale

$pCO_2 = \left(\frac{DIC \cdot H^2}{H^2 + K_1 \cdot H + K_1 \cdot K_2}\right) \cdot \frac{10^6}{K_0 \cdot FugFac}$! in µatm

$CO_2 = \frac{DIC \cdot 10^6}{1 + \frac{K_1}{H} + \frac{K_1 \cdot K_2}{H^2}}$

$HCO_3 = \frac{K_1 \cdot CO_2}{H}$

$CO_3 = \frac{K_2 \cdot HCO_3}{H}$

$Omega = \frac{Ca \cdot CO_3 \cdot 10^{-6}}{K_{ca}}$

Mis en forme : Police :Italique

Appendix B: Biogeochemical model variables and parameters

Table B1: Initial conditions of the state variables of Eco3M-CarbOx model (*diagnostic variables)

Variables	Name	Unit	values
Picophytoplankton	$PicoC$	mmolC m^{-3}	0.0480
	$PicoN$	mmolN m^{-3}	0.0092
	$PicoP$	mmolP m^{-3}	0.0003
Diatom	$DiaC$	mmolC m^{-3}	0.0571
	$DiaN$	mmolN m^{-3}	0.0089
	$DiaP$	mmolP m^{-3}	0.0007
Bacteria	$BacC$	mmolC m^{-3}	0.1083
	$BacN$	mmolN m^{-3}	0.0379
	$BacP$	mmolP m^{-3}	0.0039
DPOM **Detrital Particulate organic matter**	$DPOC$	mmolC m^{-3}	0.1252
	$DPON$	mmolN m^{-3}	0.0307
	$DPOP$	mmolP m^{-3}	0.0021
LDOM **Labile Dissolved organic matter**	$LDOC$	mmolC m^{-3}	1.0990
	$LDON$	mmolN m^{-3}	8.7980
	$LDOP$	mmolP m^{-3}	0.0018
DIM **Dissolved inorganic matter**	NH_4	mmolN m^{-3}	0.3375
	NO_3	mmolN m^{-3}	0.6723
	PO_4	mmolP m^{-3}	0.7150
	DO	mmolO m^{-3}	257.00
	DIC	µmolC kg^{-1}	2358.4
Total alkalinity	TA	µmolC kg^{-1}	2660.5
Sea water partial pressure of CO_2	pCO_2	µatm	371.28
***p*H**	*p*H	-/-	8.1099
calcium carbonate	$CaCO_3$	mmol m^{-3}	1.0000
Picophytoplankton chlorophyll*	*PicoChl*	mgChl m^{-3}	0.0193
Diatom chlorophyll*	*DiaChl*	mgChl m^{-3}	0.0229
Number of bacteria*	NBA	10^{12} cell m^{-3}	0.2000

Table B2: Balance equations of Eco3M-CarbOx model

Variables	Balance equation
Pico-phytoplankton	$\frac{\partial PicoC}{\partial t} = R_{PP}^{PicoC} - R_{resp}^{PicoC} - R_{exu}^{PicoC} - R_{Gr}$
	$\frac{\partial PicoN}{\partial t} = R_{uptPicoN}^{NH_4} + R_{uptPicoN}^{NO_3} - R_{exu}^{PicoN} - R_{Gr}$
	$\frac{\partial PicoP}{\partial t} = R_{uptPicoP}^{PO_4} - R_{exu}^{PicoP} - R_{Gr}$
	$PicoChl = Q_C^N \cdot \left(Q_{N,min}^{Chla} + f_Q \cdot \left(Q_{N,max}^{Chla} - Q_{N,min}^{Chla}\right)\right) \cdot PicoC$
Diatom	$\frac{\partial DiaC}{\partial t} = R_{PP}^{DiaC} - R_{resp}^{DiaC} - R_{exu}^{DiaC} - R_{Gr}$
	$\frac{\partial DiaN}{\partial t} = R_{uptDiaN}^{NH_4} + R_{uptDiaN}^{NO_3} - R_{exu}^{DiaN} - R_{Gr}$
	$\frac{\partial DiaP}{\partial t} = R_{uptDiaP}^{PO_4} - R_{exu}^{DiaP} - R_{Gr}$
	$DiaChl = Q_C^N \cdot \left(Q_{N,min}^{Chla} + f_Q \cdot \left(Q_{N,max}^{Chla} - Q_{N,min}^{Chla}\right)\right) \cdot DiaC$
Bacteria	$\frac{\partial BacC}{\partial t} = R_{uptBac}^{DPOC} + R_{uptBac}^{LDOC} - R_{BR} - R_{Gr}^{BacC}$
	$\frac{\partial BacN}{\partial t} = R_{uptBac}^{DPON} + R_{uptBac}^{LDON} + R_{uptBac}^{NH4} - R_{miner}^{NH4} - R_{Gr}^{BacN}$
	$\frac{\partial BacP}{\partial t} = R_{uptBac}^{DPOP} + R_{uptBac}^{LDOP} + R_{uptBac}^{PO4} - R_{miner}^{PO4} - R_{Gr}^{BacP}$
DPOM	$\frac{\partial DPOC}{\partial t} = R_{pf} + R_m - R_{Gr} - R_{uptBac}^{DPOC}$
	$\frac{\partial DPON}{\partial t} = R_{pf} + R_m - R_{Gr} - R_{uptBac}^{DPON}$
	$\frac{\partial DPOP}{\partial t} = R_{pf} + R_m - R_{Gr} - R_{uptBac}^{DPOP}$
LDOM	$\frac{\partial LDOC}{\partial t} = R_{exu}^{PicoC} + R_{exu}^{DiaC} + R_{exu}^{LDOC} - R_{uptBac}^{LDOC}$
	$\frac{\partial LDON}{\partial t} = R_{exu}^{PicoN} + R_{exu}^{DiaN} + R_{exu}^{LDON} - R_{uptBac}^{LDON}$
	$\frac{\partial LDOP}{\partial t} = R_{exu}^{PicoP} + R_{exu}^{DiaP} + R_{exu}^{LDOP} - R_{uptBac}^{LDOP}$
NH_4	$\frac{\partial NH_4}{\partial t} = R_{excr}^{NH_4} + R_{miner}^{NH_4} - R_{nit} - \sum R_{uptPhyN}^{NH_4} - R_{uptBac}^{NH_4}$
NO_3	$\frac{\partial NO_3}{\partial t} = R_{nit} - \sum R_{uptPhyN}^{NO_3}$
PO_4	$\frac{\partial PO_4}{\partial t} = R_{excr}^{PO_4} + R_{miner}^{PO_4} - \sum R_{uptPhyP}^{PO_4} - R_{uptBac}^{PO_4}$
DO	$\frac{\partial DO}{\partial t} = R_{aera} + \left(\frac{O}{C}\right) \cdot R_{PP}^{PhyC} + \left(\frac{O}{N}\right) \cdot R_{uptPhyN}^{NO_3} - \left(\frac{O}{C}\right) \cdot R_{resp}^{PhyC} - \left(\frac{O}{C}\right) \cdot R_{excr}^{DIC} - \left(\frac{O}{C}\right) \cdot R_{BR} - \left(\frac{O}{N}\right) \cdot R_{nit}$
DIC	$\frac{\partial DIC}{\partial t} = R_{aera} + R_{resp}^{PhyC} + R_{BR} + R_{excr}^{DIC} - R_{PP}^{PhyC} - R_{precip} + R_{diss}$
TA	$\frac{\partial TA}{\partial t} = 2 \cdot R_{diss} + \left(R_{uptPhyN}^{NO_3} + R_{uptPhyP}^{PO_4} - R_{uptPhyN}^{NH_4}\right) + R_{miner}^{NH_4} - 2 \cdot R_{precip} - 2.R_{nit}$

910 **Table B3: Biogeochemical processes simulated by the Eco3M-CarbOx model**

Notation	Biogeochemical processes	Unit	Formulation	
$\boldsymbol{R_{PP}^{Phy}}$	Primary production	molC m^{-3} s^{-1}	$R_{PP}^{PhyC} = P_{max} \cdot f_T^{PP} \cdot f_I \cdot PhyC$	$f_Q = min\left[f_Q^N, f_Q^P\right]; f_Q^X = \frac{Q_C^X - Q_{C,min}^X}{Q_C^X - Q_{C,min}^X + \beta_X}$ $f_T^{PP} = max\left(\frac{2\cdot(1-b)\frac{(T-T_{let})}{(T_{opt}-T_{let})}}{\left(\frac{(T-T_{let})}{(T_{opt}-T_{let})}\right)^2 - 2\cdot b\frac{(T-T_{let})}{(T_{opt}-T_{let})}+1}; 0\right)$ $f_I = \left[1 - exp\left(\frac{-\alpha_{Chla}\cdot E_{PAR}\cdot Q_C^{Chla}}{P_{max}\cdot f_Q\cdot f_T^{PP}}\right)\right]$
$\boldsymbol{R_{resp}^{Phy}}$	Phytoplankton respiration	molC m^{-3} s^{-1}	$R_{resp}^{PhyC} = k_r^{PhyC} \cdot PhyC$	
$\boldsymbol{R_{uptPhy}^{NH_4}}$	NH_4 uptake by phytoplankton	molX m^{-3} s^{-1}	$R_{uptPhyN}^{NH_4} = V_{N,max} \cdot \frac{NH_4}{NH_4 + K_{NH_4}}$	$V_{N,max} = Q_{C,max}^N \cdot R_{PP}^{Phy}$
$\boldsymbol{R_{uptPhy}^{NO_3}}$	NO_3 uptake by phytoplankton	molN m^{-3} s^{-1}	$R_{uptPhyN}^{NO_3} = V_{N,max} \cdot \frac{NO_3}{NO_3+K_{NO_3}} \cdot \left(1 - \frac{I_{in}\cdot NH_4}{NH_4+K_{in}}\right)$	
$\boldsymbol{R_{uptPhy}^{PO_4}}$	PO_4 uptake by phytoplankton	molP m^{-3} s^{-1}	$R_{uptPhyP}^{PO_4} = V_{P,max} \cdot \frac{PO_4}{PO_4 + K_{PO_4}} \cdot$	$V_{P,max} = Q_{C,max}^P \cdot R_{PP}^{Phy}$
$\boldsymbol{R_{exu}^{PhyC}}$	Phytoplankton exudation as LDOC	molC m^{-3} s^{-1}	$R_{exu}^{PhyC} = \left(1 - f_Q\right) \cdot R_{PP}^{Phy}$	
$\boldsymbol{R_{exr}^{PhyX}}$	Phytoplankton exudation as LDON or LDOP	molX m^{-3} s^{-1}	$R_{exu}^{PhyX} = \left(1 - h_Q^X\right) \cdot R_{uptX}^{Phy}$	$h_Q^X = \frac{Q_{C,max}^X - Q_C^X}{Q_{C,max}^X - Q_{C,min}^X}$
$\boldsymbol{R_{BP}}$	Bacterial production	cell m^{-3} s^{-1}	$R_{BP} = \mu_{max}^{Ba} \cdot f_Q^{Ba} \cdot f_T^{Ba} \cdot NBA$	$f_T^{Ba} = Q_{10}^{\frac{(T-T_{rem})}{10}}$; $f_Q^{BA} = min\left[1 - \frac{Q_{C,min}^{BA}}{Q_C^{BA}}, 1 - \frac{Q_{N,min}^{BA}}{Q_N^{BA}}, 1 - \frac{Q_{P,min}^{BA}}{Q_P^{BA}}\right]$
$\boldsymbol{R_{BR}}$	Bacterial respiration	molC m^{-3} s^{-1}	$R_{BR} = \rho_g^{Ba} \cdot \frac{Q_C^{Ba}}{Q_C^{Ba}} \cdot R_{BP} \cdot Q_C^{Ba} \cdot R_{BP} + \rho_r^{Ba} \cdot \left(Q_C^{Ba} - Q_{C,min}^{Ba}\right) \cdot \left(Q_C^{Ba} - Q_{C,min}^{Ba}\right) \cdot NBA$	
$\boldsymbol{R_{uptBac}^{X}}$	X uptake by bacteria	molX m^{-3} s^{-1}	$R_{uptBac}^{X} = V_{max}^{BA} \cdot \frac{X}{X+K_X^{Ba}} \cdot f_T^{Ba} \cdot NBA$	
$\boldsymbol{R_{Gr}^{Phy}}$	Phytoplankton grazing by zooplankton	molX m^{-3} s^{-1}	$R_{Gr}^{Phy} = g_{Phy} \cdot f_{Gr} \cdot Phy$	$f_{Gr} = \frac{Phy}{Phy+DPOM}$
$\boldsymbol{R_{Gr}^{DPOM}}$	DPOM grazing by zooplankton	molX m^{-3} s^{-1}	$R_{Gr}^{DPOM} = g_{DPOM} \cdot f_{Gr} \cdot DPOM$	$g_{DPOM} = \frac{g_{Pico}\cdot Pico + g_{Dia}\cdot Dia}{Pico+Dia}$; $f_{Gr} = \frac{DPOM}{Phy + DPOM}$

Tableau mis en forme

$\boldsymbol{R_{Gr}^{Bac}}$	Bacterial grazing by zooplankton	molX m^{-3} s^{-1}	$R_{Gr}^{Ba} = R_{BP} \cdot \frac{Bac}{NBA}$	
$\boldsymbol{R_{excr}^{DIM}}$	Zooplankton excretion as DIC, NH_4 and PO_4	molX m^{-3} s^{-1}	$R_{excr}^{DIM} = \varepsilon_{DIM} \cdot d_X \cdot \left(1 - k_{X,zoo}\right) \cdot \left(R_{Gr}^{Phy} + R_{Gr}^{DPOM} + R_{Gr}^{Ba}\right)$	
$\boldsymbol{R_{exu}^{LDOM}}$	Zooplankton exudation as LDOM	molX m^{-3} s^{-1}	$R_{exu}^{LDOM} = (1 - \varepsilon_{DIM}) \cdot d_X \cdot \left(1 - k_{X,zoo}\right) \cdot \left(R_{Gr}^{Phy} + R_{Gr}^{DPOM} + R_{Gr}^{Ba}\right)$	
$\boldsymbol{R_{pf}}$	Zooplankton egestion	molX m^{-3} s^{-1}	$R_{pf} = (1 - d_X) \cdot \left(R_{Gr}^{Phy} + R_{Gr}^{DPOM} + R_{Gr}^{Ba}\right)$	
$\boldsymbol{R_{m}}$	Zooplankton mortality	molX m^{-3} s^{-1}	$R_m = d_X \cdot k_{X,zoo} \cdot \left(R_{Gr}^{Phy} + R_{Gr}^{DPOM} + R_{Gr}^{Ba}\right)$	
$\boldsymbol{R_{miner}}$	Mineralization of organic matter by bacteria	molX m^{-3} s^{-1}	$R_{miner}^{X} = \left(1 - h_Q^{Ba}\right) \cdot \left(R_{uptBac}^{LDOM} + R_{uptBac}^{DPOM} + R_{uptBac}^{DIM}\right)$	
$\boldsymbol{R_{nit}}$	Nitrification	molX m^{-3} s^{-1}	$R_{nit} = k_{nit} \cdot f_T^{Ba} \cdot \frac{DO}{DO + K_{DO}} \cdot NH_4$	
$\boldsymbol{R_{diss}}$	Carbonate dissolution	molC m^{-3} s^{-1}	$R_{diss} = (1 - \Omega_C) \cdot k_{diss} \cdot [CaCO_3]$	Ω_C =aragonite saturation
$\boldsymbol{R_{precip}}$	Carbonate precipitation	molC m^{-3} s^{-1}	$R_{precip} = k_{precip} \cdot \frac{(\Omega_C - 1)}{K_C + (\Omega_C - 1)} \cdot \left(R_{PP}^{Phy} - R_{resp}^{Phy}\right)$	
$\boldsymbol{R_{aera}}$	Gas exchange with atmosphere of DO or CO_2	molX m^{-3} s^{-1}	$R_{aera} = \frac{k_{ex}}{H} \cdot ([DO]_{sea} - [DO]_{sat})$ $R_{aera} = \frac{k_{ex}}{H} \cdot \alpha \cdot \left(pCO_{2,sea} - pCO_{2,atm}\right)$	$k_{ex} = 0.31 \cdot U_{10}^2 \cdot \frac{660}{Sc}^{0.5}$ H (depth), U_{10}(wind velocity) α (solubility), Sc (Schmidt number) and $[DO]_{sat}$ are function of T and S

Table B4: Value of parameters

Parameters		Pico	Dia	Unit	Reference
P_m^C	Maximal production	1.815	1.057	d^{-1}	Sarthou et al. (2005)
m_1	Fraction of the solar energy flux photosynthetically available	0.43	0.43	-	Tett (1987)
m_2	Sea surface reflection	0.95	0.95	-	Tett (1987)
m_3	More rapid attenuation of polychromatic light near the sea surface	1.0	1.0	-	Tett (1987)
α_{Chla}	Chlorophyll-specific light absorption coefficient	$8\ 10^{-6}$	$5\ 10^{-6}$	m^2 molC $(gChla\ J)^{-1}$	Leblanc et al. (2018)
T_{opt}	Temperature optimal of growth	16.0	13.0	°C	-
T_{let}	Lethal temperature	11.0	9.0	°C	-
b	Shape factor for temperature curve	0.5	0.8	-	Lacroix and Grégoire (2002)
β_N	Coefficient in the quota function	0.0072	0.002	molN $molC^{-1}$	Leblanc et al. (2018)
β_P	Coefficient in the quota function	0.0002	0.0005	molP $molC^{-1}$	Leblanc et al. (2018)
$Q_{C,min}^N$	Minimum phytoplankton N:C ratio	0.115	0.07	molN $molC^{-1}$	Leblanc et al. (2018)
$Q_{C,max}^N$	Maximum phytoplankton N:C ratio	0.229	0.18	molN $molC^{-1}$	Leblanc et al. (2018)
$Q_{C,min}^P$	Minimum phytoplankton P:C ratio	0.0015	0.006	molP $molC^{-1}$	Auger et al. (2011); Campbell et al. (2013)
$Q_{C,max}^P$	Maximum phytoplankton P:C ratio	0.0068	0.016	molP $molC^{-1}$	Auger et al. (2011); Campbell et al. (2013)
$Q_{N,min}^{Chla}$	Minimum phytoplankton Chl:N ratio	1.0	1.0	gChl $molN^{-1}$	Leblanc et al. (2018)**
$Q_{N,max}^{Chla}$	Maximum phytoplankton Chl:N ratio	2.2	2.7	gChl $molN^{-1}$	Leblanc et al. (2018)
k_r^{PhyC}	Phytoplankton respiration rate	0.099	0.099	d^{-1}	Faure et al. (2010)
K_{NO_3}	Half saturation constant for NO_3	0.73	1.0	mmolN m^{-3}	Leblanc et al. (2018)
K_{NH_4}	Half saturation constant for NH_4	0.07	0.015	mmolN m^{-3}	Leblanc et al. (2018)
K_{PO_4}	Half saturation constant for PO_4	0.008	0.01	mmolP m^{-3}	Leblanc et al. (2018)**
I_{in}	Factor of inhibition	0.82	0.82	-	Harrison et al. (1996)
K_{in}	Amount of NH_4 from which assimilation by NO_3 is reduced.	0.578	0.578	mmolN m^{-3}	Harrison et al. (1996)
g	Grazing rate	1.452	0.846	d^{-1}	Gutiérrez-Rodríguez et al. (2011)

** calibrated from parameter used in the cited article

Mis en forme : Centré
Tableau mis en forme
Mis en forme : Centré

915 **Table B5: Value of parameters (continue)**

Parameters		Value	Unit	Reference
NBA	Number of bacteria	0.20	10^{12} cell m^{-3}	Moran (2015)
μ_{max}^{Ba}	Bacterial production rate	8.36	d^{-1}	Fraysse et al. (2013)
$Q_{C,min}^{BA}$	Minimum bacteria C:cell ratio	0.49	mmolC $(10^{12}$ cell$)^{-1}$	Fukuda et al. (1998)
$Q_{N,min}^{BA}$	Minimum bacteria N:cell ratio	0.09	mmolN $(10^{12}$ cell$)^{-1}$	Fukuda et al. (1998)
$Q_{N,max}^{BA}$	Maximum bacteria N:cell ratio	0.23	mmolN $(10^{12}$ cell$)^{-1}$	Fukuda et al. (1998)
$Q_{P,min}^{BA}$	Minimum bacteria P:cell ratio	0.005	mmolP $(10^{12}$ cell$)^{-1}$	Fraysse et al. (2013)
$Q_{P,max}^{BA}$	Maximum bacteria P:cell ratio	0.02	mmolP $(10^{12}$ cell$)^{-1}$	Fraysse et al. (2013)
ρ_g^{Ba}	Factor of carbon respired by bacteria	0.60	-	Thingstad (1987)
ρ_r^{Ba}	Respiration rate of bacteria	0.01	d^{-1}	Thingstad (1987)
$V_{DPOC,max}^{BA}$	Maximum DPOC uptake by bacteria	0.029	mmolC (~~10^{12} cell~~10^{12} cell)$^{-1}$ d^{-1}	Campbell et al. (2013)
$V_{LDOC,max}^{BA}$	Maximum LDOC uptake by bacteria	16.33	mmolC $(10^{12}$ cell$)^{-1}$ d^{-1}	Campbell et al. (2013)
$V_{DPON,max}^{BA}$	Maximum DPON uptake by bacteria	0.05	mmolN $(10^{12}$ cell$)^{-1}$ d^{-1}	Faure et al. (2010)
$V_{LDON,max}^{BA}$	Maximum LDON uptake by bacteria	0.32	mmolN $(10^{12}$ cell$)^{-1}$ d^{-1}	Faure et al. (2010)
$V_{NH_4,max}^{BA}$	Maximum NH_4 uptake by bacteria	0.32	mmolN $(10^{12}$ cell$)^{-1}$ d^{-1}	Faure et al. (2010)
$V_{DPOP,max}^{BA}$	Maximum DPOP uptake by bacteria	0.01	mmolP $(10^{12}$ cell$)^{-1}$ d^{-1}	Thingstad (1987)
$V_{LDOP,max}^{BA}$	Maximum LDOP uptake by bacteria	0.48	mmolP $(10^{12}$ cell$)^{-1}$ d^{-1}	Thingstad (1987)
$V_{PO_4,max}^{BA}$	Maximum PO_4 uptake by bacteria	0.48	mmolP $(10^{12}$ cell$)^{-1}$ d^{-1}	Thingstad (1987)
K_{DPOC}^{BA}	Half-saturation constant for DPOC	10.0	mmolC m^{-3}	Faure et al. (2010)
K_{LDOC}^{BA}	Half-saturation constant for LDOC	25.0	mmolC m^{-3}	-
K_{DPON}^{BA}	Half-saturation constant for DPON	0.50	mmolN m^{-3}	-
K_{LDON}^{BA}	Half-saturation constant for LDON	0.50	mmolN m^{-3}	-
$K_{NH_4}^{BA}$	Half-saturation constant for NH_4	0.15	mmolN m^{-3}	Leblanc et al. (2018)
K_{DPOP}^{BA}	Half-saturation constant for DPOP	0.08	mmolP m^{-3}	-
K_{LDOP}^{BA}	Half-saturation constant for LDOP	0.08	mmolP m^{-3}	Leblanc et al. (2018)
$K_{PO_4}^{BA}$	Half-saturation constant for PO_4	0.02	mmolP m^{-3}	Campbell et al. (2013)
ε_{DIC}	fraction excretion of DIC	0.31	-	Faure et al. (2010)
ε_{NH_4}	fraction excretion of NH_4	0.50	-	Faure et al. (2010)
ε_{PO_4}	Fraction excretion of PO_4	0.50	-	Fraysse et al. (2013)
d_C	Fraction of C assimilated	0.92	-	Gerber and Gerber (1979)
d_N	Fraction of N assimilated	0.95	-	Faure et al. (2010)
d_P	Fraction of P assimilated	0.95	-	Fraysse et al. (2013)
$k_{C,zoo}$	Net C growth efficiency	0.40	-	Gerber and Gerber (1979)
$k_{N,zoo}$	Net N growth efficiency	0.44	-	Le Borgne and Rodier (1997)
$k_{P,zoo}$	Net P growth efficiency	0.37	-	Le Borgne (1982)
Q_{10}	Temperature coefficient	2.0	-	-
T_{rem}	Reference temperature for mineralization	20.0	°C	-
k_{nit}	Nitrification rate	0.05	d^{-1}	Lacroix and Grégoire (2002)
T_{nit}	Reference temperature for nitrification	10.0	°C	-

Tableau mis en forme

Tableau mis en forme

Mis en forme : Centré

Mis en forme : Centré

Mis en forme : Centré

K_{DO}	Half-saturation constant DO	30.0	$mmolO_2\ m^{-3}$	Tett (1990)
k_{diss}	Dissolution rate	10.9	d^{-1}	Gehlen et al. (2007)
k_{precip}	Fraction of PIC to LPOC	0.02	-	Marty et al. (2002)
K_C	Half-saturation constant of $CaCO_3$ precipitation	0.40	$(\mu mol\ kg^{-1})^2$	
$\left(\frac{O}{C}\right)$	Ratio O:C	1.0	-	-
$\left(\frac{O}{N}\right)$	Ratio O:N	2.0	-	-

Mis en forme : Centré

Mis en forme : Centré

Appendix C: Short User Manual

After uploading the whole archive on the zenodo site (ref. doi: 10.5281/zenodo.3757677), the exact version of the Eco3M-CarbOx code used in this study can be ~~be~~ run as following:

make !two executable files will be created : eco3M_ini.exe and eco3M.exe

- the file config.ini allows to define: the time, time step, and save time of simulation variables biogeochemical process
- Results files are stocked in "SORTIES" directory
- Boundary conditions and forcings data are stocked in "DATA" directory
- All subroutines of biogeochemical processes are stocked in "F_PROCESS" directory

For further information, please contact Dr. Frédéric DIAZ (frederic.diaz@univ-amu.fr) or Dr. Christel PINAZO (christel.pinazo@univ-amu.fr)

Review of the first revised version of

"Implementation and assessment of a carbonate system model (Eco3M-CarbOxv1.1) in a highly-dynamic Mediterranean coastal site (Bay of Marseille, France)"

submitted for publication to Geoscientific Model Development

by K. Lajaunie-Salla and co-authors

General reply: We thank again the Reviewer Dr Munhoven for his second evaluation of our work. We thank too him for the detailed and useful comments that contributed to greatly improve the manuscript. We consider all of his comments to improve the manuscript.

1. General comments

The authors' reply the revised manuscript are not very "reviewer-friendly." It is nowadays standard practice to provide a "track change" (or a LATEXDIFF) version of the manuscript clearly identifying the changes made to the text, right in the text. The equivalent information is seemingly given in the reply, except that the line numbers provided there do not match, so that one has to search manually for the exact location of the changes.

The preparation of the manuscript would also have benefited from some extra care. Page numbers restart at 1 after page 23 without any apparent reason.

Reply: The preparation of the revised ms has been reviewed with care and page numbers have been reprocessed. A new check of the different sections has been carefully performed.

1.1 Appreciation of the replies to reviewers

The authors have all in all well responded to the referees' comments, with one exception though. In the response to my comment 2.3, regarding the missing effect of river intrusions on DIC — TA perturbations are taken into account, but as these are carried mainly by $HCO3^-$, they also generate DIC perturbations of the same magnitude, which are neglected — I read at the top of the fourth page (page numbers in the response would have been helpful) that

"Concerning the riverine inputs scenarii, we decide to focus on nitrate and alkalinity supply. In fact the model simulates the DIC increases, as is observed, which highlight that the carbonate system module is well resolved."

The reply to the comments is somewhat ambiguous as suggests that DIC changes are taken into account, while they are actually not, as stated in the manuscript at lines 413–414 :

" [. . .] the experimental design on the Rhône River supply only considers the TA perturbation on the carbonate system but not that due to the DIC supply."

So, even if the model reproduces the observed DIC increases (as stated in the reply), this must obviously be for the wrong reasons, as only one half of the effects of the perturbation due to river intrusions is taken into account. By the way, no one argued that the carbonate system module was not well resolved.

Reply: We decided to remove the scenario of AT supply by river and all the text referred to it in the methods and results/discussion sections. See our detailed comment on this point hereafter.

1.2 Appreciation of the revised manuscript

The model description has been improved and the rationale behind the carbonate speciation calculations is now presented in a new appendix. Unfortunately, the layout of that appendix is rather chaotic which makes it difficult to read.

2. Specific comments

2.1 River intrusion experiments: poor justification

The justification added at lines 414–417 for taking the effect of river intrusions into account only in terms of the resulting TA but not DIC perturbations is rather cavalier and scientifically untenable. This is a completely unrealistic assumption that makes the outcome of the experiment meaningless and thus essentially invalidates any conclusion drawn from it.

I only see two options to address this shortcoming:

1. the river intrusion experiments are repeated with the effect on DIC included (which should be rather straightforward to correct) and the discussion of the results adapted;

2. these experiments are simply taken out of the paper as the current results are essentially unfounded.

Even in preliminary experiments, one must not choose to disregard one of two effects of a perturbation if these are of the same order of magnitude. Such arbitrary choices lead to arbitrary results.

Reply: *We have chosen the second option proposed by the Reviewer. Mainly because it was not straightforward to consider DIC supply by River as considered for AT. In fact, DIC is not as conservative as AT is regard to salinity. It is then impossible to use a relationship between DIC and salinity as that used between AT and salinity in the previous version of our manuscript. In the context of a 0D modelling developed here, this kind of relationship would have been the only mean to take into account the DIC supply by the Rhône River. In the revised version, we stressed (l 398-401) that rivers also supply TA and DIC and a consideration for these supplies in future works may sensibly modify the modeled carbonate balance in the BoM compared to that presented in this study. Concomitantly we slightly rewrote the end of section 4.1 on the model performance in Discussion.*

As noted in the conclusion (l434), a coupling of the Eco3M-CarbOx model to a 3D hydrodynamics model is planned to better represent the complexity of functioning of the BOM. This implementation will enable, for example, to take into account actual DIC and AT supplies from the Rhône River by considering forcing values measured in the River.

3. Technical comments

Reply: All these technical comments have been taken into account in the new revised version of ms.

Page 1, line 22: “the year 2017 that is a period for which” should read “the year 2017 for which”

Page 1, line 25: “of most of variables of carbonate system except Total Alkalinity.” should read “of most of the variables of the carbonate system except for Total Alkalinity.”

Page 1, line 26: “experiments were also conducted” should read “experiments were conducted”

Page 1, line 26: “to (i) seawater” should read “to (i) a seawater”

Page 1, line 27: “Rhône River plume intrusion” should read “Rhône River plume intrusions”; by the way: the name of that river is sometimes spelled “Rhône”, more often “Rhone” — please use the same spelling consistently throughout

Page 1, line 35: “external forcing have” should read “external forcings have”

Page 5, line 188: “a salinity threshold of 37 has been chosen” – is this correct? A threshold of 37 looks rather high to me.

Page 6, line 226: “during MWC period” should read “during the MWC period”

Page 7, line 271: “15 March and 6 May” should either read “15th March and 6th May” or “March 15th and May 6th” (as on line 277, p. 8)

Page 11, line 390: “Moreover, previous study” should read “Moreover, a previous study”, or even better reformulate the sentence to read “Moreover, Fraysse et al. (2013) highlight that . . . ” and discard the citation in brackets.

Page 11, line 402: “a longer period ca. 15 days” should read “a longer period of ca. 15 days”

Page 11, lines 402–403: “high atmospheric pCO2 value and wind speed” better had to read “high atmospheric pCO2 and high wind speeds”

Page 11, line 411: “due to some two” should read “due to two”

29th and 30th pages (pages nr. 6 and 7), throughout: “in the pH scale” should read “on the pH scale”

29th page (page nr. 6): “Concentration in Total Fluoride (TF) ions” should read “Total Fluoride concentration” (without “ions,” as TF includes the non ionic HF)

29th page (page nr. 6): “Concentration in Total Sulphate (TS) ions” should read “Total Sulphate concentration” (“ions” is superfluous)

29th page (page nr. 6): “Concentration in Total Boron (TB)” should read “total boron concentration” (without “ions,” as TB includes the non ionic B(OH)3)

29th page (page nr. 6): KF is the dissociation constant of hydrogen fluoride (or of hydrofluoric acid), not of fluoride ions

29th page (page nr. 6): in the expression for KF, the exponent for Ions should be 0.5 (or 1/2) and not 1.5.

30th page (page nr. 7): “Every constant are corrected by the hydrostatic pressure” should read “All the constants are corrected for the effect of hydrostatic pressure”

Guy Munhoven

Liège, 9th October 2020